

BUILDING A COST EFFICIENT DIGITAL RADIOGRAPHY SYSTEM FOR
EDUCATIONAL PURPOSES

By

CHRIS BROWN

Bachelor of Science

Henderson State University

Arkadelphia, Arkansas

2010

Submitted to the Faculty of the
Graduate College of the
Oklahoma State University
In partial fulfillment of
The requirement for
The Degree of
MASTER OF SCIENCE
JULY 2013

BUILDING A COST EFFICIENT DIGITAL RADIOGRAPHY SYSTEM FOR
EDUCATIONAL PURPOSES

Thesis Approved:

Jerimy Polf

Thesis Advisor

Eric Benton

Committee Member

Stephen Mckeever

Committee Member

ACKNOWLEDGEMENTS

I would like to thank my advisor, Dr. Jerimy Polf for his unwavering patience, guidance, and support that kept me going throughout this project. Without his plentiful insight, I would have had an immensely difficult time piecing together this project. Dr. Polf kept me on track when I would want to deviate from putting in the work to complete the mission at hand. I would also like to thank Patrick Paul for his amazing carpentry skills in helping build the housing unit for the Digital Radiography System. Another thank you goes out to Jared Giem for taking part in the brainstorming process in regards to help with the Labview programming.

I would like to thank Dr. Benton for his unique style of teaching. I came into graduate school overwhelmed and under-committed. It was he who quickly put me in my place and showed me that anything you do in life (even homework) ought to be done with a sense of pride and professionalism.

I would like to thank my wife, Kimberly Brown for whom without her, graduate school would not have been possible. Her love and support has kept me focused on the task at hand.

I cannot thank my parents enough for helping me get my college education started by scraping enough money together to send me to my first semester of college. Their combination of love and support has helped me through the challenging periods of my educational career.

Finally, I would like to thank the OSU machine shop for helping cut the lead and wood to appropriate sizes to build this Digital Radiography System and Dr. Mckeever for his support in the project.

Name: CHRISTOPHER GLEN BROWN

Date of Degree: July, 2013

Title of Study: BUILDING A COST EFFICIENT DIGITAL RADIOGRAPHY SYSTEM FOR EDUCATIONAL PURPOSES

Major Field: Physics with Option in Medical Physics

ABSTRACT:

Due to the growing need for Medical Physicists, many universities are implementing a Medical Physics program into their academic catalog. To help establish a new program, feasible equipment may be needed to help academic departments provide a hands-on experience for students and help teach the basic concepts of Medical Physics. For example, clinical Digital Radiography Systems (DRS) are used to help teach the basic concepts of digital imaging. However, such systems can cost in excess of \$100,000, creating a financial obstacle that will be difficult to overcome. Hence, the development of a cost efficient digital radiography system may be desired in order to eliminate the financial obstacle and give students a hands-on learning experience. This DRS uses three main components to develop an image, an x-ray source, an intensifying plate, and a charge-coupled device (CCD) camera. All three components are housed in a lead-lined box. The purpose of this project is to find the limitations of our DRS and compare the price between our DRS and commercially available DRSs. At optimal settings, a SNR of 25 is shown across the intensifying screen that can identify objects as small as 0.42mm. A Contrast-detail phantom shows the ability to decipher the varying thickness of foam rubber squares. The total cost of our DRS comes to ~\$17,000.00, a fractional price tag compared to a commercially available DRS.

TABLE OF CONTENTS

Chapter	Page
LIST OF TABLE AND FIGURES.....	vi
1 INTRODUCTION.....	1
1.1 Brief History of Radiography.....	1
1.2 Purpose of this Project.....	5
2 PHYSICS OF DIGITALRADIOGRAPHY.....	7
2.1 Overview of Digital Radiography Systems.....	7
2.1.1 X-ray Source.....	7
2.1.2 X-ray Detection.....	12
2.1.3 Digital Image Construction.....	20
3 CONSTRUCTING AN EDUCATION DIGITAL RADIOGRAPHY SYSTEM.....	21
3.1 Educational DRS	21
3.1.1 DRS Housing.....	22
3.1.2 Safety Measures.....	26
3.1.3 DRS Core Components.....	26
3.1.4 Image Processing.....	27
3.2 Characterizing the DRS.....	30
3.2.1 Noise.....	30
3.2.2 Contrast.....	33
3.2.3 Spatial Resolution.....	34
4 RESULTS AND DISCUSSION.....	38
4.1 Noise Results.....	38

4.2 Spatial Resolution Results.....	41
4.3 Contrast Results.....	46
4.4 Combining the Three Tests.....	48
5 CONCLUSION.....	54
5.1 Goal of this Project.....	54
5.2 Cost of DRS.....	55
5.3 Building a More Cost Efficient DRS.....	55
5.4 Future Work.....	57
6 REFERENCES.....	59

List of Tables

Table 2-1: How phosphor size, layer thickness, and phosphor concentration of intensifying screens affects resolution, dose, and density	18
Table 3-1: As signal increases, relative noise decreases and SNR increases.....	31

List of Figures

Figure 1-1: First radiograph of Mrs. Roentgen's hand.....	1
Figure 1-2: Typical set-up for film radiography	3
Figure 1-3: Process of a Digital Radiography System	3
Figure 2-1: Simplistic diagram of x-ray source	8
Figure 2-2: How Bremsstrahlung occurs	9
Figure 2-3: How characteristic x-rays occur	10
Figure 2-4: Characteristic x-ray electron binding energies of different shells.....	11
Figure 2-5: Film cassette.....	13
Figure 2-6: Direct and indirect methods of detecting x-rays and converting to a digital image..	13
Figure 2-7: X-rays interacting through an object via Photoelectric effect and Compton Scattering.....	15
Figure 2-8: Probability of Photoelectric and Compton Scattering occurring in different tissue, bone, Lead and, NaI.....	16
Figure 2-9: Mass attenuation coefficient as a function of energy for Photoelectric and Compton interactions in lead, tissue, and Iodine.....	16
Figure 2-10: Cross-section of an intensifying screen.....	18
Figure 2-11: Reflective layer of intensifying screen	19
Figure 3-1: Inside view of our educational Digital Radiography System.....	21

Figure 3-2: Frame of our Digital Radiography System.....	22
Figure 3-3: Photon energies of I-125 and Cr-51.....	24
Figure 3-4: Aerial view of Digital Radiography System's lid.....	25
Figure 3-5: Lead sandwiched between wood panel for the lid.....	25
Figure 3-6: Diagram of the set-up of our Digital Radiography System.....	27
Figure 3-7: Profile of both the background image and the subtraction of dark noise from the background image.....	28
Figure 3-8: Corrected image if intensifying screen.....	29
Figure 3-9: Isometric display of noise.....	32
Figure 3-10: How noise measurements were taken.....	33
Figure 3-11: How contrast measurements were taken.....	34
Figure 3-12: Line pair phantom example.....	35
Figure 3-13: Concept of spatial frequency.....	36
Figure 3-14: Fan-like line pair phantom.....	37
Figure 4-1: How noise measurements were taken.....	39
Figure 4-2: Measurements of SNR at 50kV.....	39
Figure 4-3: Measurements of SNR at 30kV.....	40
Figure 4-4: Measurements of SNR at 10kV.....	40
Figure 4-5: Image of line pair phantom at 50kV/79 μ A.....	42
Figure 4-6: Measurements of MTF at 50kV/79 μ A, 20 second exposure.....	42
Figure 4-7: Image of line pair phantom at 30kV/79 μ A.....	44
Figure 4-8: Image of line pair phantom at 20kV/79 μ A.....	44
Figure 4-9: Measurements of MTF at 50-30-20kV/79 μ A, 20 second exposure.....	45

Figure 4-10: Contrast-detail phantom image at 50-30-20kV/79 μ A, 20 second exposure.....	47
Figure 4-11: Contrast measurements of 50-30-20kV/79 μ A, 20 second exposure.....	47
Figure 4-12: Two example (Pistol Pete and a Motherboard) objects to be imaged by our DRS..	48
Figure 4-13: Pistol Pete image measurements of 50-30-10kV/79 μ A, 20 second exposure.....	49
Figure 4-14: Pistol Pete image measurements of 50-30-10kV/79 μ A, 10 second exposure.....	50
Figure 4-15: Motherboard image measurements of 50-30-10kV/79 μ A, 20 second exposure.....	52
Figure 4-16: Motherboard image measurements of 50-30-10kV/79 μ A, 10 second exposure.....	53
Figure 5-1: Cheaper x-ray source found through Ebay.....	56
Figure 5-1: Cheaper CCD camera found through Amazon.....	56

Chapter 1: Designing a Low Cost Digital Imaging System

1.1 Brief History of Radiography

In Germany in 1895, Willhelm Roentgen stumbled upon the discovery of x-rays when he was experimenting with cathode rays (electron beams) and soon after, produced the world's first radiographic image (Figure 1-1). While conducting research using Crooke's tubes, a barium platinocyanide screen (which was within eyesight of Roentgen) began fluorescing while cathode rays were being emitted in the Crooke's tube. The glowing screen showed Roentgen that something (x-rays) originating from the Crook's tube must be interacting with the chemical make-up of this screen (Hill, 1975). This x-ray luminescence phenomenon helped quickly lead to the development of radiography. The combination of the fluorescing screen and film gave way to the first radiography system.



Figure 1-1: The first radiograph taken of Roentgen's wife in 1895. As one can see, the contrast of different substances (bone, ring, fat) is due to the attenuation of x-rays through Mrs. Roentgen's hand and ring (USNLM, 2012).

The ability to use x-rays, which attenuate through different materials at different rates, has revolutionized patient care. The benefits of using x-rays for imaging (easily produced, low cost, noninvasive, etc...) were immediately apparent and radiography systems were implemented into hospitals soon after their discovery by Roentgen. Radiography systems have become the foundation for diagnosing many different injuries and diseases that occur inside the body. Along with radiography's obvious benefits, comes the risk of using radiation safely. As time has passed, it has been shown that dealing with the radiation output of such systems can be dangerous and should be handled with the upmost of care. The duty of supervising the radiation output of different medical devices in a hospital fall onto the shoulders of a Medical Physicist.

Two standard types of radiographic imaging are used for medical imaging: screen film radiography (SFR) and a digital radiography system (DRS). Standard screen-film radiography (Figure 1-2) uses a cassette made of film sandwiched between two intensifying plates. The x-ray beam is first attenuated by the object/patient being imaged. The beam then interacts with the intensifying plates creating visible light and causing the sandwiched film to darken, forming an image; however, the image that is formed on the film is not complete. Additional chemical processing is needed in order to fully develop the film and fix the final image. With a DRS, the film cassette is replaced by a digital receptor (Figure 1-3). This digital receptor measures the x-ray beam intensity after it passes through the object/patient being imaged. The measured data is then read and processed by specialized digital imaging software to produce the final image. This final, corrected image is projected on the display control. Image processing is where the advantage of DRSs comes into play. The digital information in the image can be manipulated by digital imaging software allowing users to vary the characteristics of the digital images and to extract needed information from the image that would be otherwise unnoticeable.

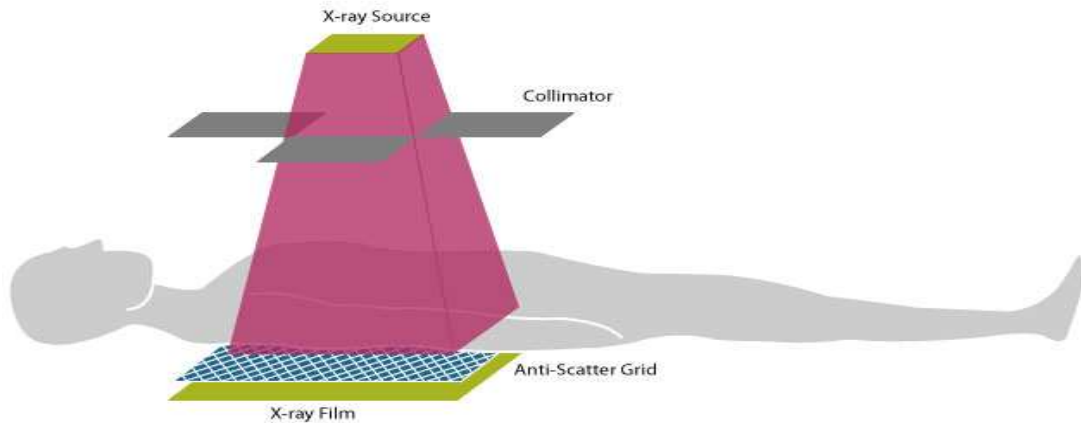


Figure 1-2: A typical setup for a screen-film radiography system. The film is sent to be developed into an image after being exposed (Siemens).

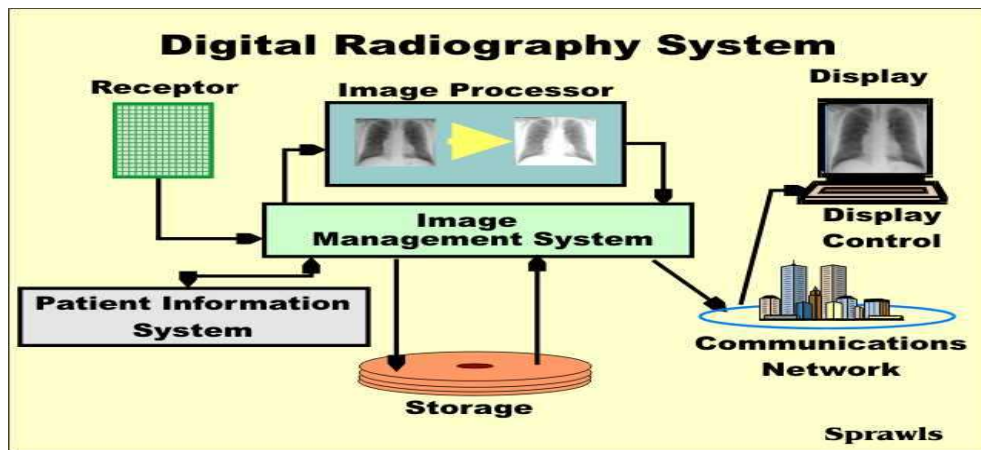


Figure 1-3: The x-rays strike the detector (receptor) and are converted into a digital intensity value matrix. An image processor then assigns grayscale values to the matrix so it can be displayed as an image. This image is then saved to a file for easy retrieval. Once the image is saved, it can be sent to any network dubbed appropriate with a simple click of the button (Sprawls).

After the image is processed, the image is then stored as digital data, for quick and easy retrieval. The images may then be easily shared among different locations across communication networks.

As recently as 2008, the majority of health clinics still used screen-film based radiography (van der Stelt, 2008). If hospitals have already invested the time, money, and effort into a SFR system, they may not want to deal with the upfront cost of a DRS. However, if a health care facility is newly built and looking for a radiography system to purchase, DRS would be the favored choice. In recent years, health care facilities have begun rapidly switching to digital radiography systems due to the same reason associated with building an educational digital radiography system: first, fixed non-linear grey scale response, SFR is limited to a fixed dose latitude, and limited potential for reducing dose to the patient (Bansal, 2006). While this is a beneficial reason for a clinical setting to switch to DRS, an educational DRS would not use a patient for imaging; therefore, limiting dose to the object would only be a secondary concern for system design. Second, DRSS enhances the quality of an image over film radiography. For example, images taken from a DRS can be mathematically filtered to bring out key features in an image. Third, film needs to be processed with hazardous chemicals to develop and fix the image. A DRS will get rid of these chemicals along with time and space required in processing the film. Fourth, film can only be used once; consequently, if the film is lost, damaged, or poorly developed, another image must be taken. These errors can cost a facility time and money, while costing a patient time and delivering additional dose for unnecessary reasons. Finally, after the film has been developed, space is needed for storage. A system then needs to be set up for easy retrieval of the stored film. A DRS will eliminate the clutter of a file room and make retrieval of images much faster and convenient with a simple click of a button. On top of easy retrieval,

sending images to a different location (facility to facility) will be as simple as sending an e-mail. These limitations of SFR can be a hassle, costing time, money, and safety. As stated above, dose does not come into effect when choosing an educational radiography system, but keeping up with the technological advances of the future is necessary for educational programs.

1.2 Purpose of this Project

Many universities are adding Medical Physics programs into their academic catalog due to the growing need for Medical Physicists. To help establish a new program, feasible equipment may be needed to help academic departments provide a hands-on experience for students and help teach the basic concepts of Medical Physics. Clinical digital radiography systems are used to help teach the basic concepts of digital imaging. However, such systems can cost in excess of \$100,000, creating a financial obstacle that will be extremely difficult for a university to overcome. For example, Absolute Medical Equipment sells a Source-Ray SR-130D/55G Direct digital portable X-Ray System for \$118,745, a price tag that is well above the limits of most academic physics departments. Hence, the development of a cost efficient digital radiography system is desired that can eliminate the financial obstacle and give students a hands-on learning experience. Along with being cost efficient, the system design needs to be capable of producing images with adequate characteristics concerning noise, spatial resolution, and contrast.

The raw components of a digital radiography system are commonly found within existing labs in academic Physics and Engineering departments or are readily available for consumer purchase. If items such as a CCD camera, intensifying screen, or x-ray source are not already available in the department, then one can easily purchase these components via the internet or local electronic store for a reasonable price. The purpose of this Masters of Science project was

to construct a working educational DRS from component pieces that were either readily available in the Oklahoma State University department of Physics or could be easily purchased.

Chapter 2 – Physics of Digital Radiography

2.1 Overview of Digital Radiography Systems

All radiography systems have two pieces of equipment in common, an x-ray source and a detector. These two items are used in different ways in order to capture an image. Generally, all x-ray sources used in radiography systems behave in the same way. The difference in x-ray sources in radiography systems is the capacity of voltage and current supplied to the source. On the other hand, detecting x-rays can be done in a variety of ways to produce an image. Using the different characteristics of different detectors lets one set up a variety of radiography systems. However, a DRS set-up becomes advantageous when wanting to extract a variety of different information from the same image and wanting to gather that information quickly.

2.1.1 X-ray Source

X-rays are created by bombarding a dense piece of metal (anode), such as tungsten (Figure 2-1) with high energy electrons. This bombardment of electrons causes two different types of x-ray reactions to occur. First, most of the incident electrons interact by traveling through an atom and coming into close contact with the nucleus. Once the electrons approach the nucleus, they are attracted to each other due to the opposing forces of the nucleus (positive) and electrons (negative). The nuclear force field causes the electron to slow down, change course, and lose energy. The decelerating electrons emit a spectrum of x-rays known as bremsstrahlung (Figure 2-2). The energy of the x-ray photon that is created from the

deceleration of the incident electron is the difference between the electron's energy entering and exiting the tungsten atom. Second, the electrons may collide with the tungsten's electron cloud and ionize an electron from the inner shell. As the electron is ejected from the inner-shell, a higher orbiting electron will come to fill the void space. This creates a cascade of electrons filling in the void shells from the different orbits. In the act of filling the ionized electron shell, a characteristic x-ray is emitted. The energy of the characteristic x-rays are equal to the difference of binding energies of the filled shells (Figures 2-3, 2-4). Even though the two target interactions occur, diagnostic x-ray tubes are very inefficient by wasting 99% of the incident electron energy on heat. Only about one percent of target interactions that occur produce x-ray photons.

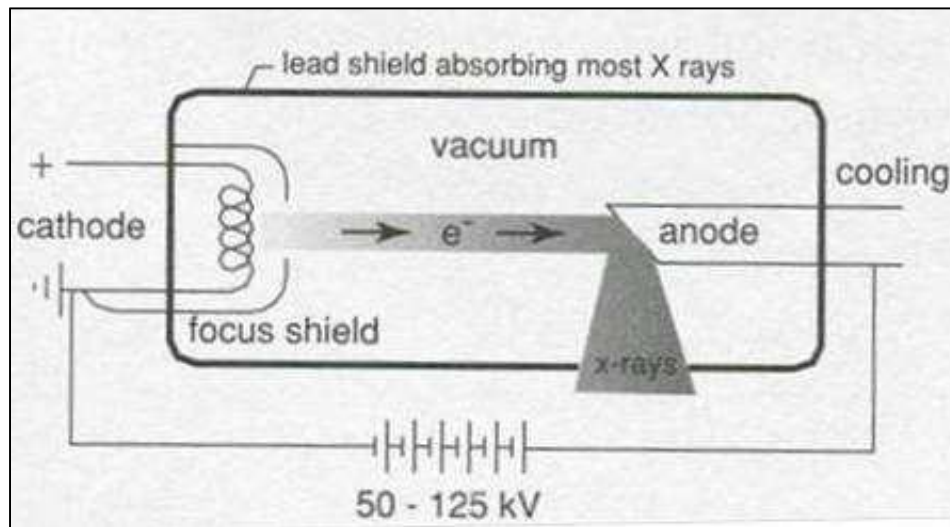


Figure 2-1: Simplistic diagram of an x-ray source. (Suetens, 2002)

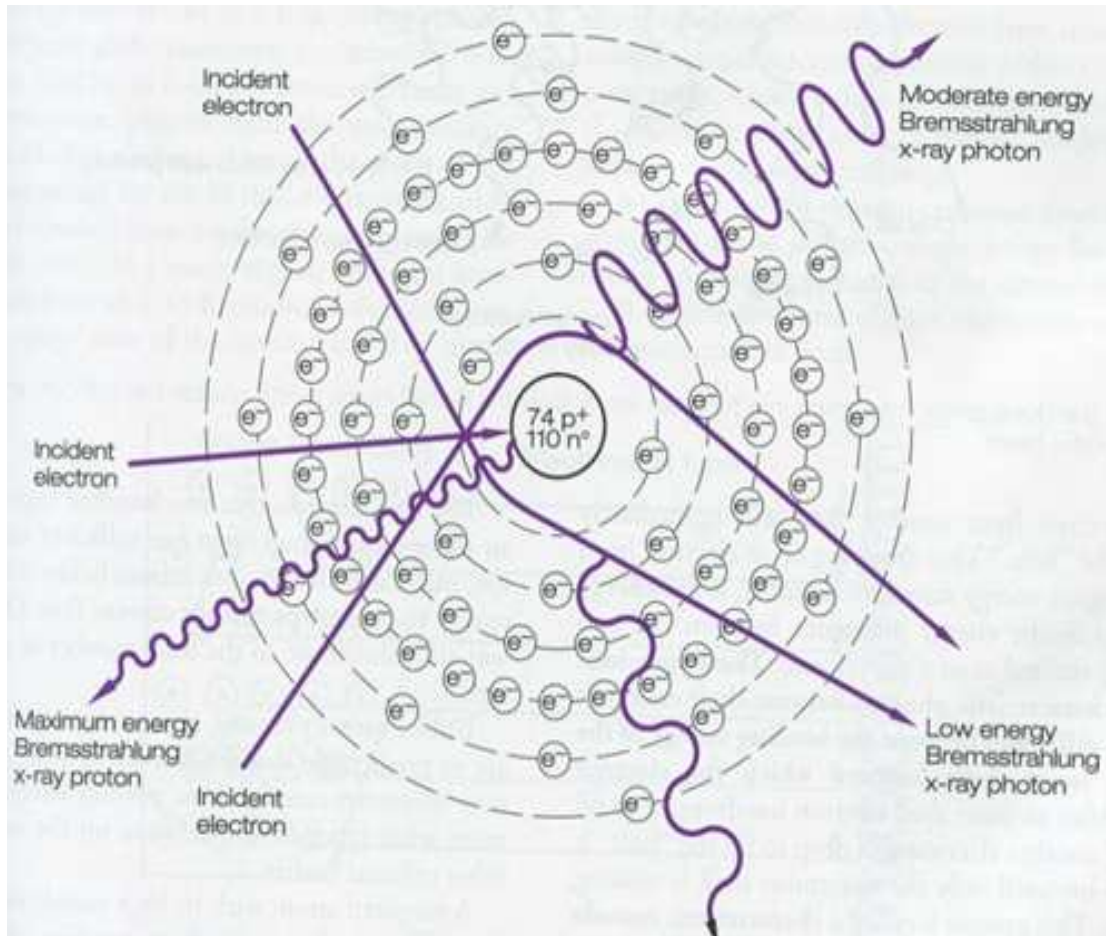


Figure 2-2: The incident electrons enter the tungsten atom and approach the nucleus. The nucleus “brakes” the electrons and sends them on a different course. The “braking” of the electrons causes a loss of energy and results in a spectrum of x-rays. (Carlton, 2001)

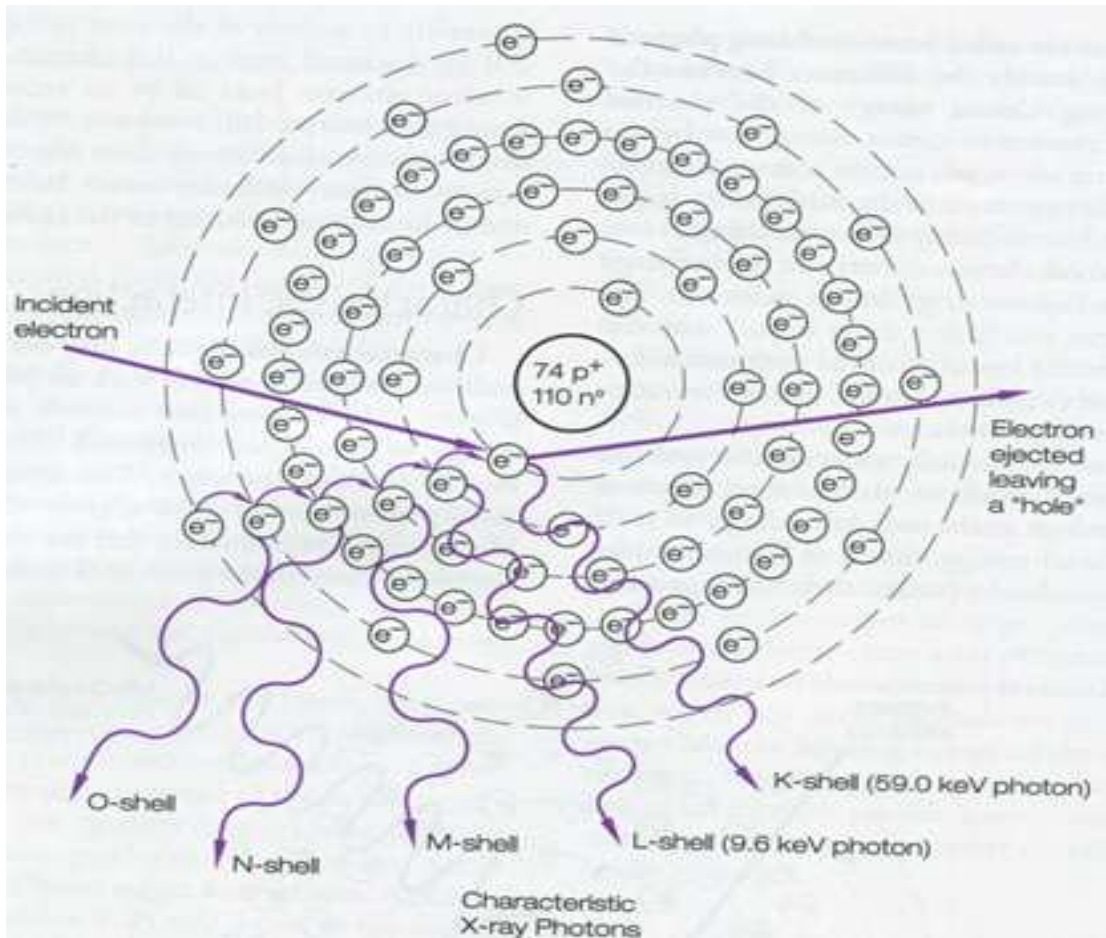


Figure 2-3: The incident electron collides with the electron cloud of the tungsten. The collision ionizes an electron of a particular shell. The ionization causes higher orbiting electrons in the cloud to replace the ionized electron, thus creating a characteristic x-ray. (Carlton, 2001)

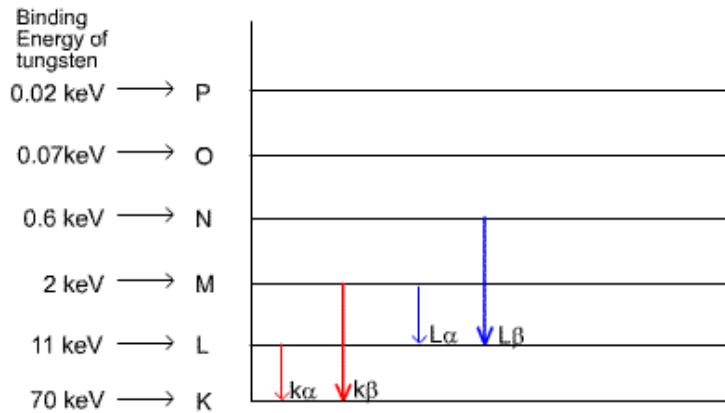


Figure 2-4: The binding energy differences between the different shells of an atom (Griffiths).

The two settings that control the output of the x-ray source are voltage and the filament current. The voltage applied between the anode and cathode of the x-ray tube accelerates the electrons toward the anode target. As the potential between the anode and cathode increases, the accelerating force felt by the electron increases, resulting in an increased electron energy striking the target and an increased maximum in the energy of the x-rays emitted. As the x-ray energy is increased, the penetrating capability of the x-ray is increased. In addition to the high voltage across the x-ray tube, a separate voltage is applied across the cathode filament. This voltage produces a current in the filament (cathode), which dictates the number of electrons available to be accelerated to the anode. As the current flows through the filament, it heats up, resulting in electrons being “boiled off” for acceleration. As the filament current increases, more electrons are boiled off and accelerated, which in turn increases the number of x-rays produced.

2.1.2 X-ray Detection

Several different x-ray detectors have been used for radiographic imaging. Photographic film was first used by Roentgen with the addition of intensifying screens. The photographic film is a strip of transparent plastic that has been coated on one side with microscopically small silver halide crystals. The silver halide crystals begin to darken when exposed to light. The film is inserted into a cassette with two intensifying screens as show in Figure 2-5. Once the cassette is exposed to x-rays, the x-rays penetrate the cassette, strike the intensifying screens, the intensifying screens convert the x-rays into visible light, and the light strikes the film. Once an appropriate x-ray exposure has been delivered, the film displays various amounts of information about the object that is being imaged.

Other x-ray detectors that use electronic detection can be divided into two classes, direct and indirect detection. Direct methods convert x-rays into an electric charge without using a medium. The x-rays strike a photoconductor (such as selenium or silicon) directly and are converted into an electric charge which in return is digitized into an intensity matrix and converted into an image. Indirect methods use a medium, such as a scintillator, that convert the incident x-rays into visible or ultraviolet light that can be detected by a CCD or photodiode, as shown in Figure 2-6 (Chotas, 1999). Whether the direct or indirect method is used, images can be produced instantaneously when converting the detected x-rays to a digital image.



Figure 2-5: A typical cassette composed of two intensifying screens inside of a light-tight container. The film is inserted between the screens and closed. The x-rays penetrate the cassette, strike the intensifying screens, and are collected onto the film by way of visible light from the screens.

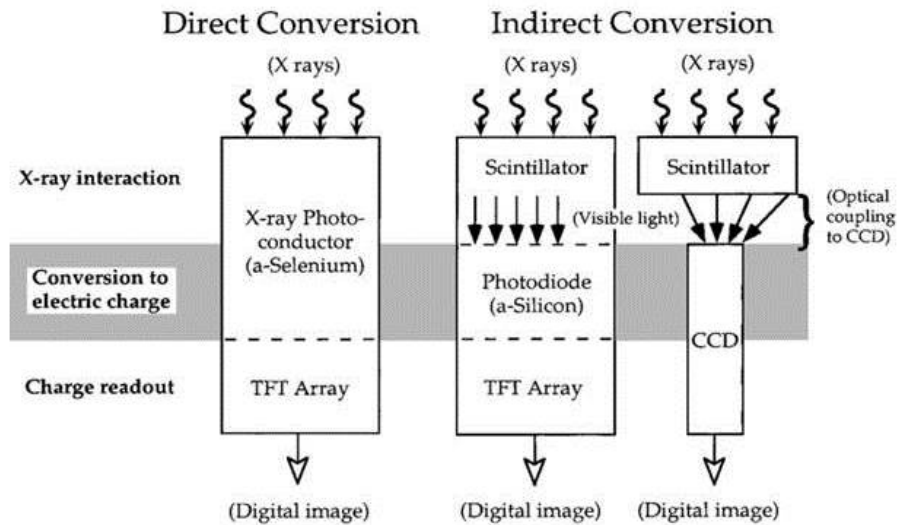


Figure 2-6: A comparison of direct and indirect methods used when detecting x-rays and converting them into a digital image. Direct method uses a photoconductor that converts the x-rays into an electric charge with no transitional stage. Indirect methods use some form of medium that converts the incident x-rays into a different wavelength, such as visible light, which in return can be detected by other forms of detectors (Chotas, 1999).

For radiographic imaging, the x-ray beam is directed at an object located on a stand in front of an x-ray detector. X-ray energies used in typical radiography systems are anywhere from 15-150 keV. As the beam penetrates an object, x-rays are able to pass through the object with no interactions, or interact via three different processes (Figure 2-7). These three x-ray interactions in radiographic imaging are as follows: photoelectric effect, Compton scattering, and pair production. Since radiographic x-rays have maximum energies below the threshold for pair production (1.022 MeV), it can be ruled out as an interaction process. Photoelectric and Compton split the probability of x-ray interactions. At lower photon energies, photoelectric interactions are predominant due to the fact that the photon energies are closer to the electron binding energies of different materials. As the energy increases, Compton scattering begins to become the principal interaction as seen in Figure 2-8. However, Compton scattering attenuates photons of different composition at roughly the same rate since it is nearly independent of Z ($\frac{1}{h\nu}$), while the photoelectric effect is proportional to both Z and energy ($\frac{Z^3}{h\nu^3}$) (Bushberg et al., 2002). Figure 2-9 shows how each interaction attenuates incident photons for different materials.

Given that Compton scattering is present in virtually every radiographic procedure, scattered x-ray photons will occur within the imaged object. These scattered photons are not wanted in radiographic imaging since they can blur images. Nonetheless, x-rays from the imaging beam strike the object, and different regions of the beam are attenuated at different rates due to the density and atomic composition of the object. For example, the human body is composed of bone, fat, water, and muscle; all of which vary in density and composition and attenuate an x-ray beam differently. This varying attenuation provides us with information needed to produce an image of the densities and compositions of tissues in the body without need for surgery.

After the x-ray beam passes through the object being imaged, it strikes an x-ray detector. The detector used in our system is an intensifying screen, originally used for film radiography. Rather than use the addition of film with the intensifying screens, the screens are removed from the cassette and used solely for their ability to convert x-rays into the visible light spectrum. The film itself is relatively insensitive to radiation; hence, more x-rays are needed to properly expose the film to produce a quality image (Bushberg, 2002). Although film is able to be directly exposed with x-rays and gives the highest resolution possible, intensifying screens are used diagnostically to decrease the dose delivered to patients and can create a higher contrast image.

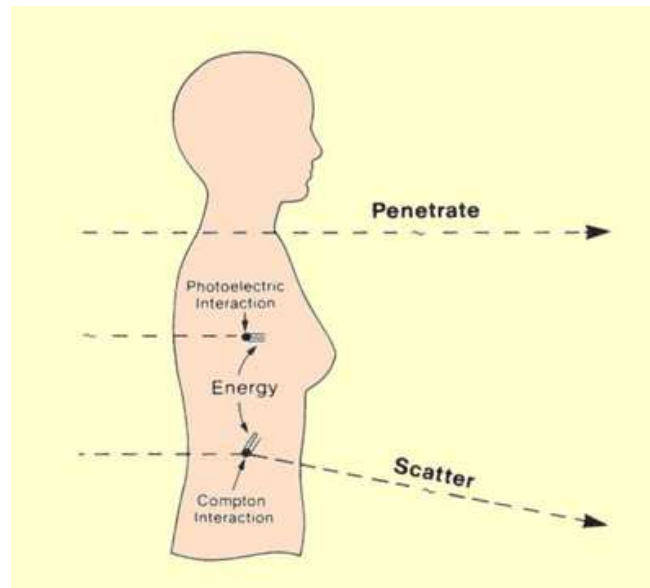


Figure 2-7: As incident x-ray photons interact in the body, some will be able to pass through without interacting, while other will interact in the body via photoelectric effect and/or Compton scattering (Sprawls).

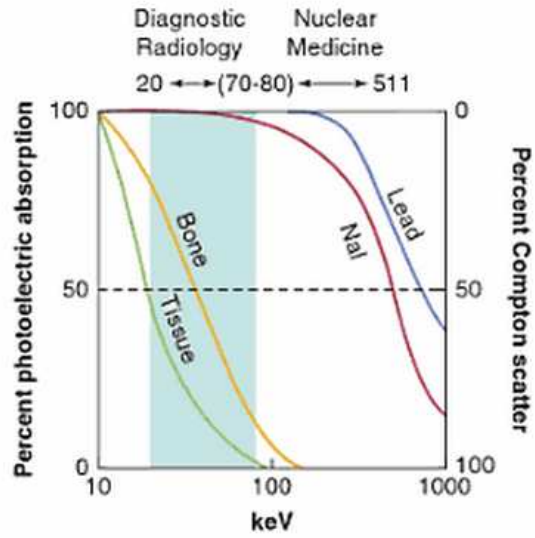


Figure 2-8: The probability of a Compton and photoelectric interaction changes as a function of photon energy (Bushberg et al., 2002).

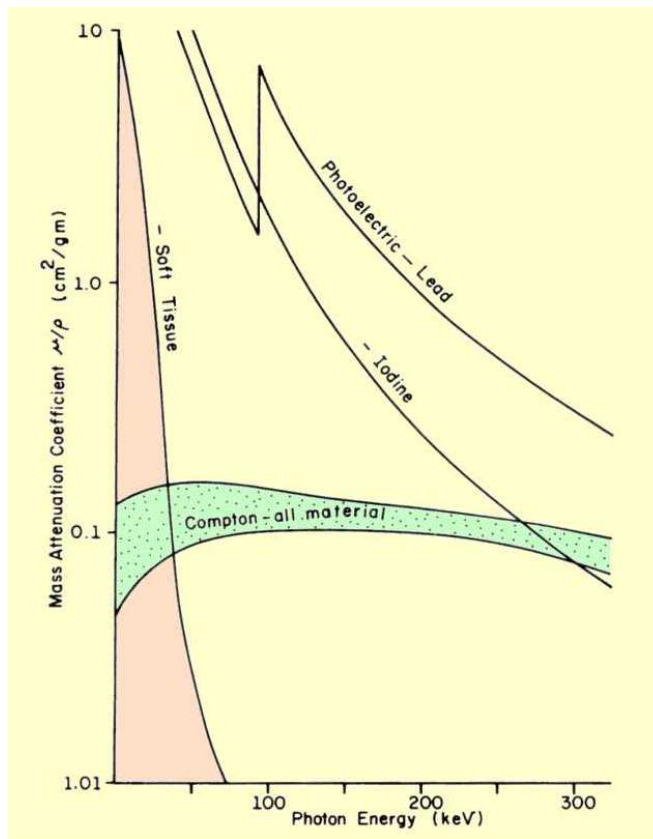


Figure 2-9: At approximately 30 keV, the probability of Compton scattering and the photoelectric effect are split evenly (Sprawls).

The three factors for the resolving power of intensifying screens are phosphor layer thickness, phosphor size, and phosphor concentration of the intensifying screen (Carlton, 2001). The resolution effects of intensifying screens can be seen in Table 2-1. A typical intensifying screen is made of four main components: phosphor, base, reflective layer, and a protective coating (Figure 2-10). Phosphors absorb x-ray energy and emit visible light. The phosphors absorb the initial energy which causes the electrons of the phosphor atom to “jump” to an excited state. Since the electrons want to be in their ground state, they fall from this excited state back to their original ground state by emitting a visible photon. If the process of relaxing from the excited state is fast ($\sim 1/100,000$ of a second), then the process is called fluorescence (Oldnall, 1999). The phosphor layer is where the physical interactions take place, converting x-rays to visible light. A high atomic number is preferred when using phosphors to help increase the probability of an interaction by the incident x-rays. The base is typically made of a polyester plastic, coated with phosphors that will absorb the incident x-ray energy. The most important function of the base is to be radiolucent. This allows the transference of x-rays to the phosphor without scattering them, which it turn creates artifacts in the image. When the x-ray photons hit the phosphors, light is emitted isotropically. To preserve the visible light, the reflective layer reflects the visible photons back into one direction (Figure 2-11). A protective plastic coat is then applied to the top of the phosphor layer. This protective coat mainly helps keep the phosphors from being damaged. Since the screens have to be handled physically, the protective coat stops scratches, abrasions, stains etc... (Carlton, 2001).

Phosphor Change	Effect on Image Resolution	Effect on Patient Dose	Effect on Density
<i>Phosphor size</i>			
Increases	Decreases	Decreases	Increases
Decreases	Increases	Increases	Decreases
<i>Layer Thickness</i>			
Increases	Decreases	Decreases	Increases
Decreases	Increases	Increases	Decreases
<i>Phosphor concentration (Packing Density)</i>			
Increases	Increases	Decreases	Increases
Decreases	Decreases	Increases	Decreases

Table 2-1: The benefit of increasing the phosphor size, layer thickness, and phosphor concentration is that it will increase the odds of incident x-ray photons interacting with the phosphors. This helps the dose distribution since the more x-rays that interact with the phosphors, the more light output there will be from the intensifying screen. However, a give and take is needed to produce a quality image and a safe dose distribution for patients (Carlton, 2001).

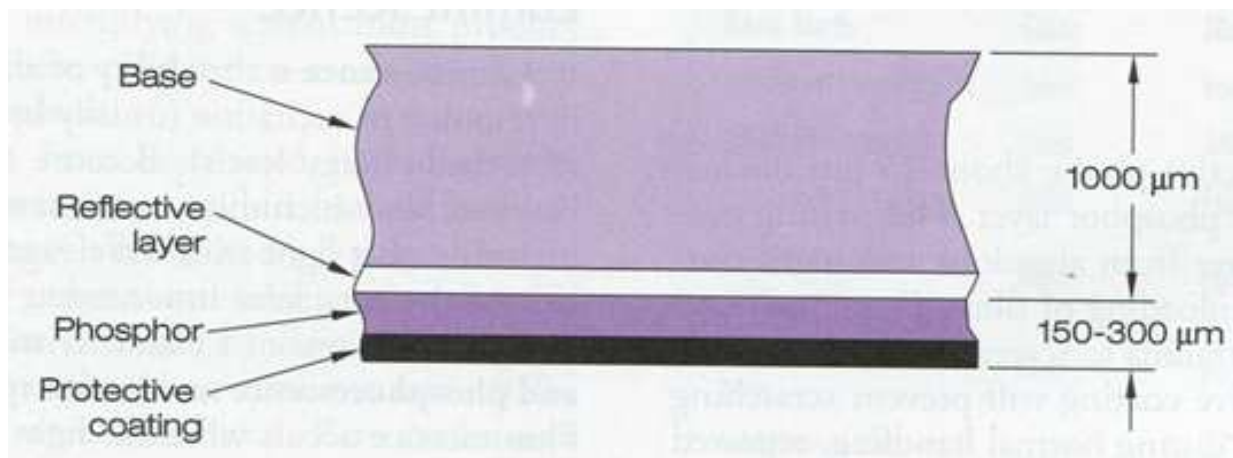


Figure 2-10: Cross-section of an intensifying screen (Carlton, 2001).

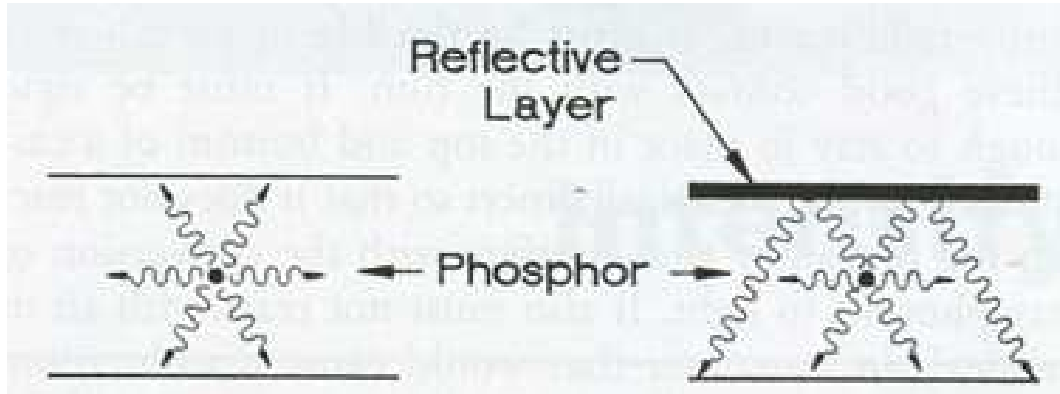


Figure 2-11: The reflective layer of intensifying screens directing the visible light photons in the correct direction (Carlton, 2001).

During most of the 20th century, calcium tungstate phosphors were used for intensifying screens. However, rare earth phosphors such as gadolinium oxysulfide (Gd_2O_2S) have taken over due to the enhanced conversion efficiency of x-ray to visible light (~5% and ~15% respectively). The rare-earth phosphors have higher atomic numbers (57-71), resulting in a higher x-ray interaction cross-section. The intensity of light output by the intensifying screen is directly related to the intensity of incident x-rays that come in contact with the screen. Hence, the more efficient the screen is at converting x-rays to visible light, the fewer x-rays needed to produce an image and thus the reduction of dose delivered to a patient. Therefore, screens should detect as many x-rays as possible for a more efficient radiograph (Bushberg, 2002).

2.1.3 Digital Image Construction

As the incident x-rays are attenuated in an object, different intensity values of the x-rays are detected to produce an image. This collection of varying intensity x-rays are converted to an electric charge and digitized to an intensity matrix. Each element of the matrix is then assigned a grayscale value for the purpose of displaying the final image. An image relies on three distinct properties to gather as much information as possible: noise, spatial resolution, and contrast. The unique aspect about digital imaging is the fact that digital images are able to be manipulated. When an image is captured on film, there is nothing that can be done after developing to help improve different aspects of that image. Since a digital image is basically a matrix of different intensity values, it can be mathematically altered to enhance different characteristics. Characteristics include magnification, varying contrast, or clarity. Portions of an image can be enhanced so that specific information can be extracted. The ability to manipulate images gives digital radiography the possibility of extracting more information from a single image than SFR.

Chapter 3 – Constructing an Educational Digital Radiography System

3.1 Educational DRS

The core components for this educational DRS include an x-ray source, intensifying plate, and a CCD camera as a detector, as shown in Figure 3-1. Since x-rays are a type of ionizing radiation, the x-ray source must be encompassed in a lead-lined housing unit. Additional software must be used (not pictured) to help acquire and correct the images produced by the CCD camera.

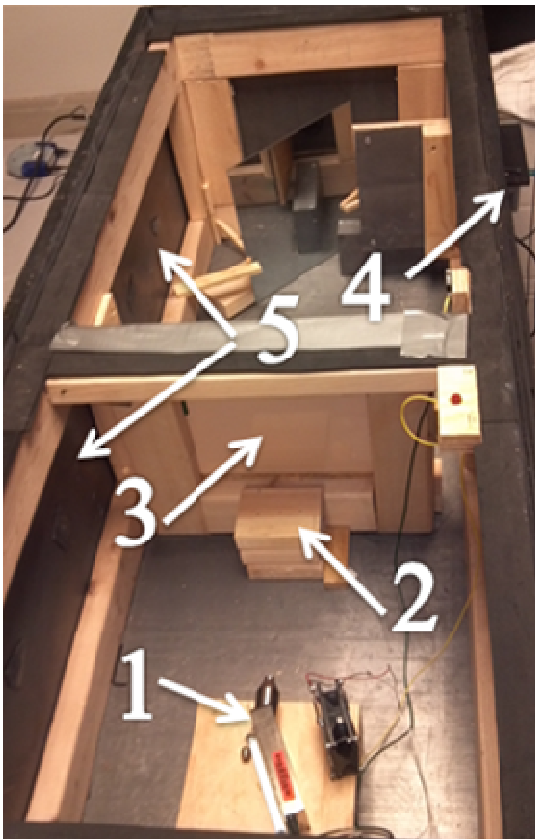


Figure 3-1: An Inside view of the educational digital radiography system set-up.

- 1) X-ray source.
- 2) Object stand.
- 3) Intensifying screen.
- 4) CCD camera.
- 5) Lead shielding.

3.1.1 DRS Housing

The DRS needed to be large enough to contain all digital radiography components, yet small enough to be easily accessible. A surplus table (28''x 59'') located in the lab was determined to be the size needed for the DRS. Thus, an educational tabletop DRS was constructed to be used for classes such as "Introduction to Medical Imaging." The frame was first put together using eighteen 2x4s of different length purchased from a local hardware store. They were screwed together using standard metallic decking screws. Once the frame was built, plywood panels with attached lead sheeting were then secured to the outside of the frame (Figure 3-2). This was done as a means of shielding the users from primary and scattered x-rays. The lead used was 1/8 inch thick, enough to stop 99.99% of all x-rays emitted from the 50kV source.

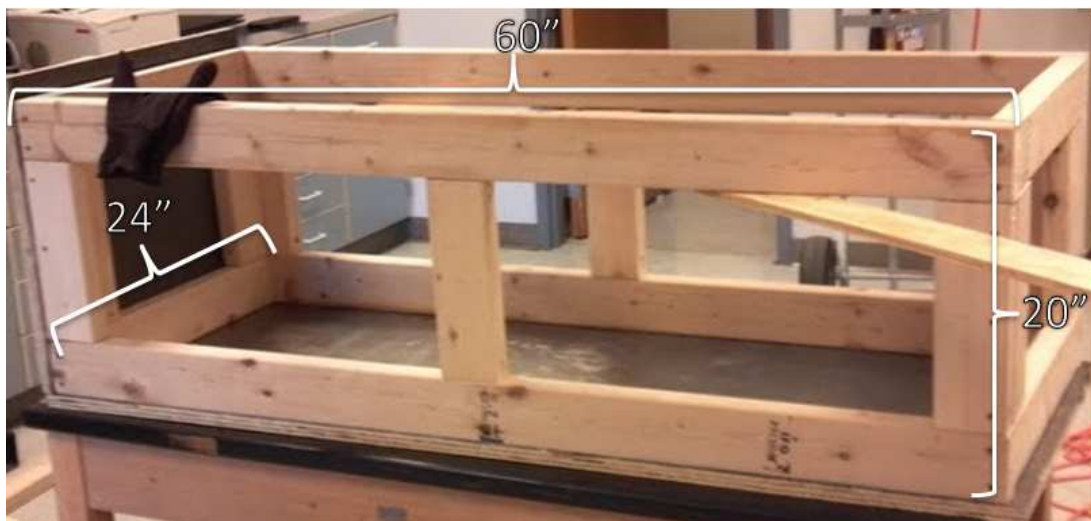


Figure 3-2: The frame dimensions posted above are with the lead panels attached. The lead panels are attached to the outside of the frame as shown above.

The thickness of lead needed to stop 99.99% of x-rays can be calculated using the following equation:

$$\frac{I}{I_0} = e^{-\mu x}$$

where $\frac{I}{I_0}$ is the fraction of x-rays that escape the lead shielding, μ is the attenuation coefficient, and x is the lead thickness. According to the National Institute of Standards and Technology (NIST), a 50keV energy x-ray has the mass attenuation coefficient (μ_m) of $730.4 \frac{\text{cm}^2}{\text{g}}$. Using the relationship of μ_m and lead's density ($\rho = 11.3 \frac{\text{g}}{\text{cm}^3}$), we find that:

$$\mu = \mu_m * \rho = \frac{8253.52}{\text{cm}}$$

Therefore, using the above equation and an attenuated intensity ratio of $\frac{I}{I_0} = 0.0001$, the thickness of lead (x) needed to shield for 50 keV x-rays is $x = 0.00112\text{cm}$ or 0.0004 inches. Thus, $1/8$ inch (0.125 inch) of lead shielding far exceeds the thickness required for most incident x-rays. Since the max energy of the x-ray spectrum is 50keV, $1/8$ inch of lead shielding far exceeds the amount of shielding needed to stop 99.99% of incident x-rays.

Nevertheless, radiation protection protocols are put in place by different radiation safety committees to help keep both the public and occupational workers as safe as possible.

“Introduction to Radiation Safety for Research Personnel” for Oklahoma State University states that a minimum of $1/8$ inch of lead must be used for low energy photon sources such as Cr-51 and I-125 as shown in Figure 3-3. Approximately $1 \mu\text{rem}/\text{hour}$ was measured by the OSU radiation safety officer outside the housing unit for the DRS, which complies with the $2 \text{mrem}/\text{hour}$ limit that is enforced by the OSU radiation safety manual. We found that this minimum shielding requirement was adequate to shield for the 50 keV maximum x-ray energy

emitted from our source. Therefore, the shielding for the housing of our DRS system was found to meet and exceed institutional requirements of shielding low energy x-rays.

27 of 27 Monoenergetic Electrons				No Beta Transitions			
20 of 20 Photons				No Alpha Particles			
ICODE	Radiation	Intensity	Energy (MeV)	ICODE	Radiation	Intensity	Energy (MeV)
2	X ray	1.77E-03	3.34E-03	2	X ray	1.47E-04	4.46E-04
2	X ray	1.15E-03	3.61E-03	2	X ray	5.85E-05	5.11E-04
2	X ray	6.15E-03	3.76E-03	2	X ray	5.27E-04	5.11E-04
2	X ray	5.52E-02	3.77E-03	2	X ray	9.22E-06	5.13E-04
2	X ray	3.58E-02	4.03E-03	2	X ray	2.85E-04	5.18E-04
2	X ray	4.96E-03	4.07E-03	2	X ray	3.29E-05	5.90E-04
2	X ray	8.18E-03	4.12E-03	2	X ray	6.24E-05	5.90E-04
2	X ray	4.19E-04	4.17E-03	2	X ray	3.09E-08	4.84E-03
2	X ray	9.94E-03	4.30E-03	2	X ray	6.70E-02	4.94E-03
2	X ray	4.55E-03	4.57E-03	2	X ray	1.33E-01	4.95E-03
2	X ray	1.85E-03	4.83E-03	2	X ray	8.88E-03	5.43E-03
2	X ray	1.08E-03	4.83E-03	2	X ray	1.76E-02	5.43E-03
2	X ray	3.16E-05	2.69E-02	2	X ray	2.89E-06	5.46E-03
2	X ray	3.98E-01	2.72E-02	1	Gamma ray	9.83E-02	3.20E-01
2	X ray	7.41E-01	2.75E-02				
2	X ray	7.20E-02	3.09E-02				
2	X ray	1.40E-01	3.10E-02				
2	X ray	1.44E-03	3.12E-02				
2	X ray	4.30E-02	3.17E-02				
1	Gamma ray	6.67E-02	3.55E-02				

Figure 3-3: The tables for I-125 (left) and Cr-51 (right) give the different photon energies that are emitted from these sources. These energies are on the range of about 30 keV which is very close to max energy of the source used in the DRS (USNRC, 2006).

The lid to the housing unit was cut into two portions to lighten the load when opening the unit. Hinges were attached to the portion of the lid that overlooked the x-ray source and object stand. A lead window (approximately equivalent to 1/8 inch of lead) was also inserted into the lid, as shown in Figure 3-4. The design of the lid consisted of a 1/8 inch thick piece of lead sandwiched between 2 sheets of plywood, as shown in Figure 3-5.

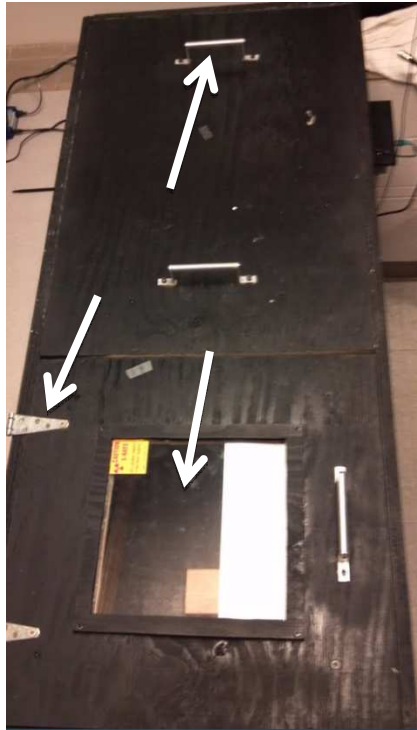


Figure 3-4: Hinges and handles were added to help open the heavy, lead lined lid. The portion of the lid that uses hinges to open is roughly 1/3 the length of the lid. The lead window gave an easy view of the object stand to make sure everything is in place, once the lid was closed.



Figure 3-5: The lead was sandwiched between two wooden panels for the lid.

3.1.2 Safety Measures

In order to operate any x-ray source, safety precautions need to be taken to avoid confusion and accidental exposure. To ensure that everyone in proximity to the source knows that x-ray source is in use, two different stimuli must be present. In this case, a blinking caution light and an audible beeping noise are used when the x-ray source is in operation. Anyone that is near the DRS will be able to hear the noise and see the flashing caution light when the source is in use. Another precautionary step that is taken is adding interlocks. Since the lid to the DRS has two different entries, two interlocks were placed just underneath each lid. These interlocks prevent the x-ray source from operating if either section of the lid is open or being opened. Additionally, a precautionary "do not cross" parameter was set up approximately two feet from the DRS while the x-ray source is in operation.

3.1.3 DRS Core Components

The DRS uses a MINI-X Miniature X-ray Tube, made by Amptek. The range of voltage and current are 5-50kV and 10-200 μ A respectively. The maximum combination of voltage and current is 50kV/79 μ A. The x-ray tube is directed towards the object stand located at the center of the housing unit and directly in front of an intensifying screen. The intensifying screen was taken from a Dupont Cronex 10" X 12" Xtra Life Intensifying Screens X-Ray Film Cassette. Instead of putting a film inside the cassette to capture an image, an intensifying screen was removed from the cassette and placed in the center of the DRS housing unit. During the absorption of x-ray energy, the visible light emitted from the intensifying screen must be captured and saved to create the radiographic image. For our DRS, a CCD camera is used to capture the incoming light from the intensifying screen. In order to prevent the camera from being exposed to ionizing

radiation, the set-up in Figure 3-6 was used. The camera used with our system is a Luca S EMCCD produced by Andor Technology. Attached to the Luca S is a Japan Computar TV Lens with an f-number of 1.4.

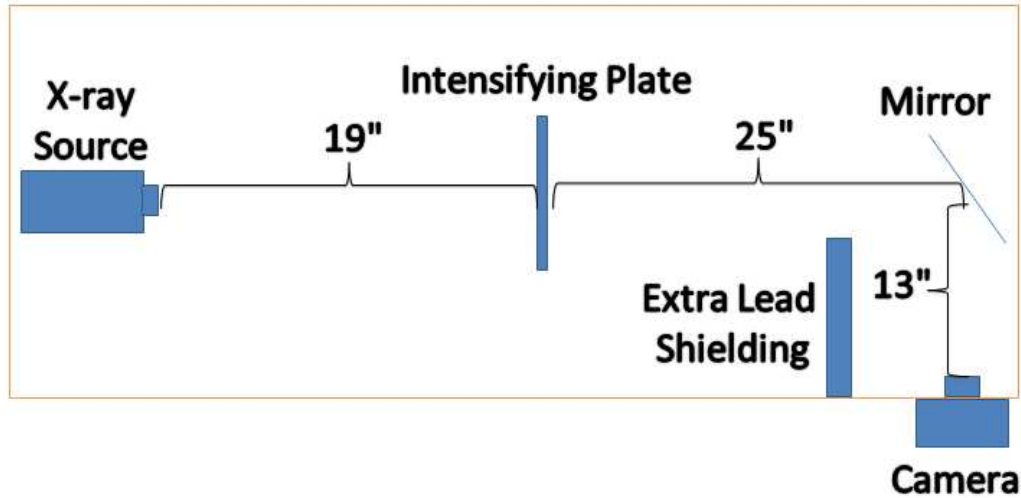


Figure 3-6: Diagram of educational DRS. The placement of the camera was used in order to avoid the circuitry being hit by ionizing radiation.

3.1.4 Image Processing

Once the image data has been captured and digitized by the CCD camera, it is loaded into an image pre-processing program written with the Labview data acquisition software. This image pre-processing program is used to correct for any characteristics of the images arising due to the components of the system and not due to attenuation of the x-ray beam in the imaged object. For instance, electronic noise in the CCD camera occurs in each element of the CCD chip. As an image is being acquired, this so-called “dark noise” results in randomly located spikes in the

pixel data. In order to remove the dark noise from a final acquired image, several “dark images” ($D(x,y)$) must be acquired without the x-ray source operating (a completely dark environment). All acquired $D(x,y)$ images are averaged together, and then subtracted from the raw background image (acquired by the CCD camera (Figure 3-7)). This raw background image is taken without any objects present. A dark noise subtracted image $G'(x,y)$ is produced according to the relationship

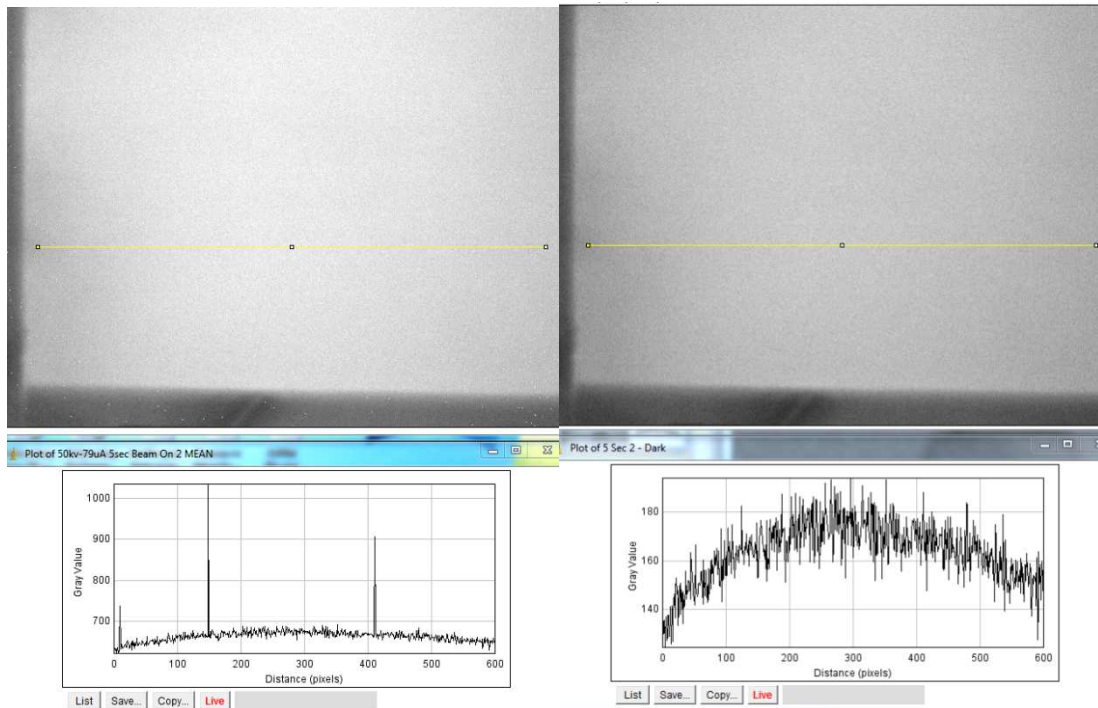


Figure 3-7: The image on the left shows the random dark noise that occurs when using a CCD camera. The image on the right has been corrected by subtracting the dark image from the raw background image. However, the arc in the plot profile from the $G'(x,y)$ remains due to the non-uniform light output by the intensifying screen.

Ideally, the intensifying screen should produce a uniform intensity across its entire surface when irradiated. However, as shown in Figure 3-7, correcting for the dark noise does not produce a uniform image profile. Therefore, further corrections need to be made to the $G'(x,y)$ images. Due to the physical condition and age of the intensifying screen (dating back to the 1970's), it is reasonable to believe that intensity of visible photons is not uniform across the entire screen. In order to correct for this, the below equation may be used:

Where $I(x,y)$ is the final corrected image of an object and $I_{\text{raw}}(x,y)$ is the raw image data of an object measured by the CCD camera. Using this procedure produces a final image with a uniform response across the entire surface of the image, as shown in Figure 3-8.

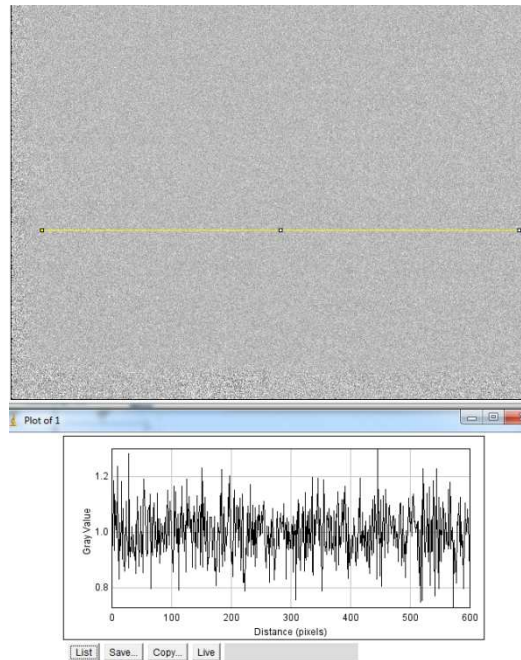


Figure 3-8: By using the above equations, the image has been corrected by eliminating the noise present with CCD cameras and non-uniform light output of the intensifying screen.

After correcting the image in the image processing programs, the image is saved as a 2D matrix of pixel intensity values. A program called ImageJ (NIH, 2013) is then used to convert this pixel intensity matrix back into a grayscale image. This is done by taking the pixel intensity values and applying a grayscale transformation. For instance, an 8-bit image is composed of an allowed pixel value range (0-256). When a pixel with a value of 0 is displayed, it is set to black. Pixels with a value of 256 are set to white and pixels in between 0-256 are set to a specific shade of gray.

3.2 Characterizing the DRS

Ideally, in a medical setting, every image taken from a DRS should contain enough information for a physician to make highly educated diagnoses. In order to characterize the DRS, three different quantities need to be measured: noise, contrast, and spatial resolution. These three elements of a DRS are crucial to understanding the information that can be extracted from a DRS image. However, due to the characteristic contrast, noise, and spatial resolution of each DRS, the total information that can be extracted by the physician may vary. Therefore, knowing and understanding these quantities for each individual DRS is extremely important.

3.2.1 Noise

Noise is a stochastic component of an image. It can originate from several different locations, such as the analog to digital conversion of an image, random fluctuations from the x-ray source, or random fluctuations in the cameras electronic components. This random background signal is detected but does not add to the quality of an image. It can most closely be associated with the static “white noise” heard when switching between different radio stations

(Carlton, 2001). The standard deviation (noise) can be denoted as (thanks to the Poisson distribution):

$$\sigma = \sqrt{N}$$

where N is the mean number of photons per pixel. Relative noise is what is perceived in an image by a human observer. This noise is also called coefficient of variance (COV) and denoted by:

$$\text{Relative Noise} = \text{COV} = \frac{\sigma}{N}$$

The inverse of COV is what is known as the signal-to-noise ratio and given by:

$$\text{SNR} = \frac{N}{\sigma} = \frac{N}{\sqrt{N}} = \sqrt{N}$$

As N increases, the noise (σ) will increase as well, but at a slower rate. Table 3-1 shows that as photons increase per pixel, the SNR will increase due to the noise increasing at a slower rate than N (Bushberg et al., 2002).

Photons/Pixel (N)	Noise (σ) ($\sigma = \sqrt{N}$)	Relative Noise (σ/N) (%)	SNR (N/σ)
10	3.2	32	3.2
100	10	10	10
1,000	31.6	3.2	32
10,000	100	1.0	100
100,000	316.2	0.3	316

Table 3-1: As N increases, the SNR increases thus giving a better quality image (Bushberg 2002).

The quantity SNR is used to measure ratio of signal compared to noise. A high SNR signifies little noise can be seen in the image while a SNR below 5 deems objects in the image are not 100% discernible. This SNR limit of 5 is known as Rose's Criterion (Bushberg et al., 2002). In Figure 3-9, the concept of noise is shown through an isometric display. In order to evaluate the noise levels of the educational DRS, nine different sections of an intensifying screen image were recorded as shown in Figure 3-10. The noise in the images produced by our DRS is the standard deviation of the signal. The noise in each of these sections was then analyzed to determine the noise levels across the entire image acquired with our educational DRS.

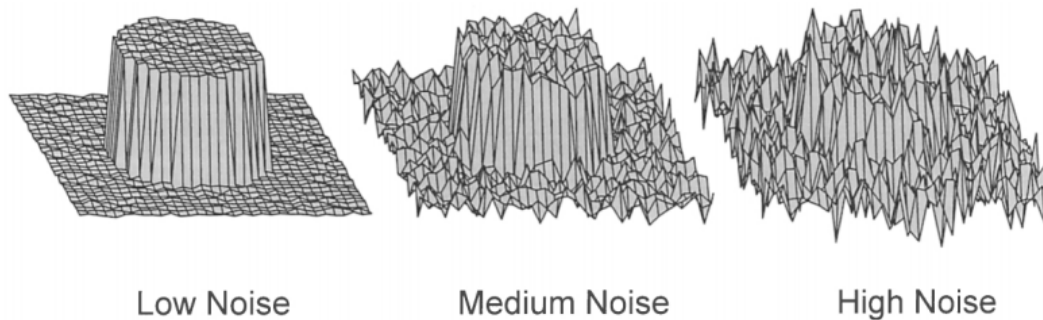


Figure 3-9: As the SNR decreases, the object in question becomes more difficult to distinguish. In medical imaging, the difficulty in distinguishing an image due to noise can result in a physician not being able to accurately diagnose patients or miss vital information (Bushberg, 2002).

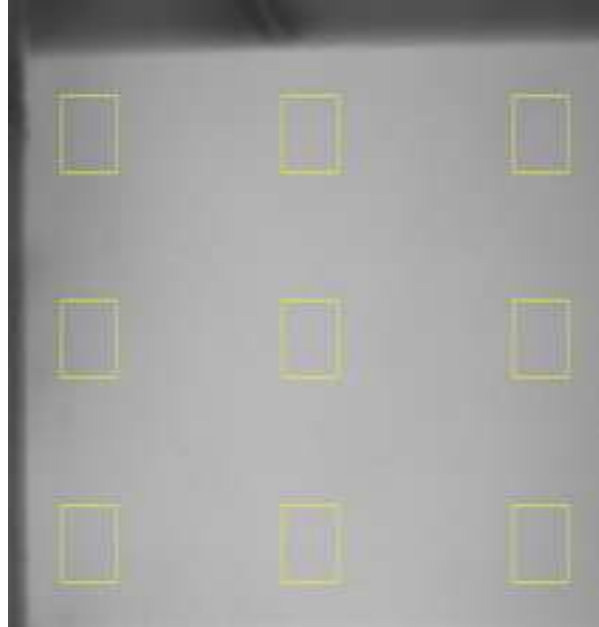


Figure 3-10: The noise was measured in each yellow box across the intensifying screen.

3.2.2 Contrast

The ability to distinguish between various substances in a radiograph is important when gathering pertinent information. For example, the body is composed of many different components that attenuate x-rays at different rates (fat, muscle, air, bone, etc...). Therefore, the ability to characterize a DRS to identify which pixel values are associated with the different density components of the body is beneficial. To characterize the contrast in our educational DRS, we imaged a sheet of paper with foam rubber squares of varying thickness and size as shown in Figure 3-11. We then evaluated how the contrast in the image changed as a function of the size and thickness of the foam rubber squares. This allowed us to evaluate the limitations in object size and thickness that could be accurately identified within images taken with our educational DRS.

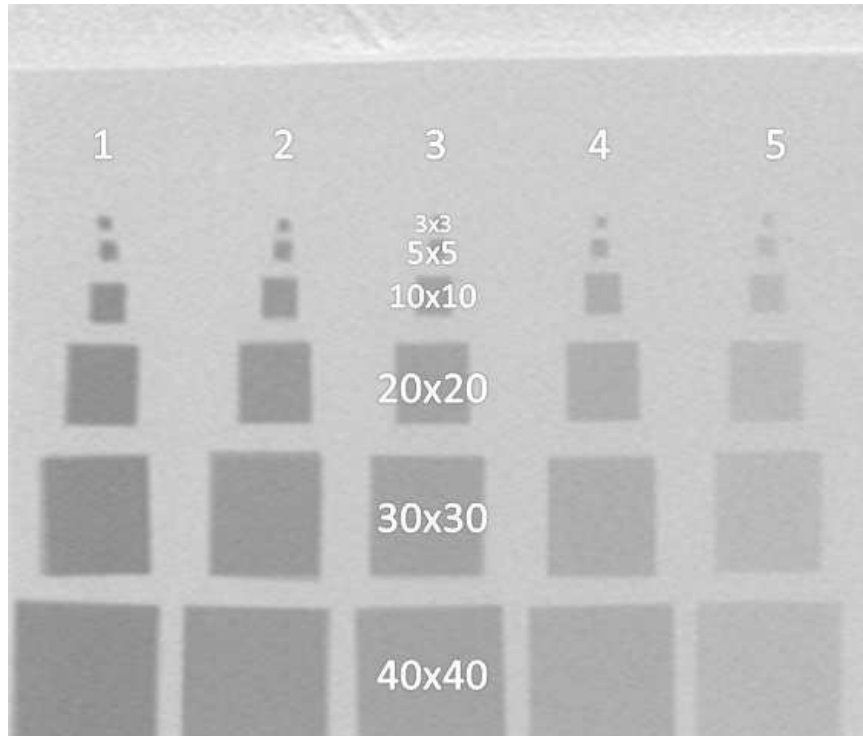


Figure 3-11: The foam squares are attached to a piece of copy paper by generic stick glue. Column 1 begins at a thickness of 10mm and decreases by 2mm each column thereafter. Square sizes are in millimeters.

3.2.3 Spatial Resolution

Finally, we need to understand the limitations on how small of an object that can be accurately identified in images taken with our DRS. This can be measured using a “line pair phantom” that contains a series of parallel lines with decreasing distance between them as shown in Figure 3-12. This increasing spatial frequency is often measured in line pairs (LP) per unit length (e.g. LP/mm). In the case of our DRS, spatial frequency is measured in LP/mm. It is a useful way to express the resolution of an imaging system. A simple way to relate line pairs to spatial frequency is to think of a sound wave and temporal frequency. As the sound waves begin to be separated by shorter periods of time, the frequency of each wave will increase (Figure 3-13). Similarly to the distance between line pairs, as objects become closer together, the spatial

frequency increases. As the line pairs continue getting closer together, they become harder to differentiate on an image.

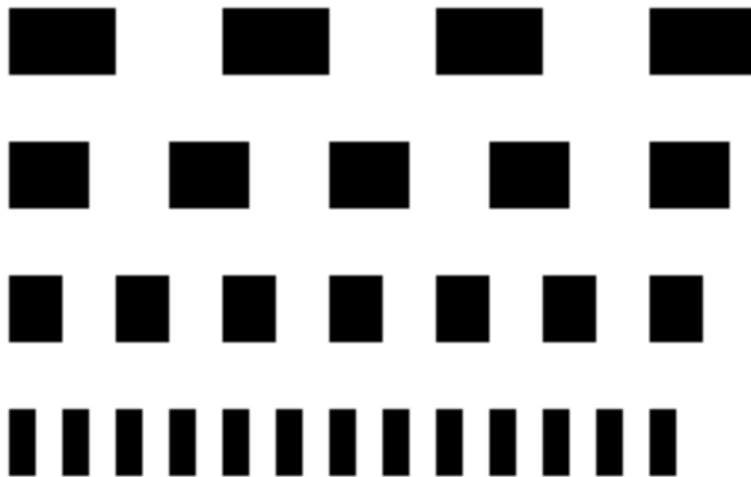


Figure 3-12: A line pair phantom slowly increasing its spatial frequency of line pairs. A line pair consists of both the black and white squares together. Therefore, the first row has four line pairs and the last row has thirteen line pairs.

Once spatial frequency reaches the point at which they can no longer be distinguished as two separate lines, we can then define this as the upper limit of spatial resolution for our DRS. Spatial resolution for a DRS is often measured by determining the modulation of the line pair phantom and is given by:

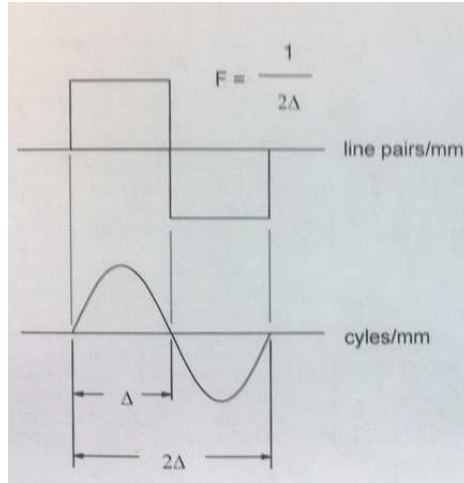


Figure 3-13: The concept of spatial frequency given by a sine wave. Δ indicates half of a sine wave; therefore, in order to find the frequency of any spatial domain: Frequency (F) = $\frac{1}{2\Delta}$ (Bushberg et al., 2002).

As the line pairs move closer in proximity, the Modulation of the image gray scale value decreases until the line pairs are unable to be differentiated as two separate lines. This modulation is often normalized to the value obtained for $f = 0$ (lines infinitely spaced), Modulation(0), where the normalized maximum value is 1. This normalized Modulation value is known as the Modulation Transfer Function (MTF) and is given by the relationship (MMD, 2012):

$$\text{MTF}(f) = \frac{\text{Modulation}(f)}{\text{Modulation}(0)}$$

For testing of our DRS, we used a phantom with line pairs cut into a copper plate (produced by the OSU Physics department machine shop) and a commercial line pair phantom made by Fluke Biomedical. Instead of vertical line pairs as shown in Figure 3-12, the

commercial line pair phantom contained a fan-like pattern (as seen in Figure 3-14) for determining the resolution of the system.



Figure 3-14: A fan-like line pair phantom that has the boundaries of 0.5-5 LP/mm.

Chapter 4 – Results and Discussion

4.1 Noise Results

As shown in Figure 4-1 (and Figure 3-10), nine separate sections of the intensifying plate were analyzed and the median signal (gray scale value) and noise (standard deviation) were measured. Rose's Criterion (Bushberg et al., 2002) states that at a SNR of 5 or greater for an object in the image will be discernible from the image background with a 100 % probability. When the background SNR of an imaging system falls below 5, it is possible that some objects in the image (especially low contrast objects) may not be easily discernible. This results in a loss of information that could be extracted from the image. Therefore, any image taken that has a background SNR above 5 will satisfy Rose's Criterion and produce an image from which accurate information can be extracted. The goal of the noise study is to find the lower limits of both the x-ray energy and beam current at which our DRS will produce images with a background SNR value that satisfies Rose's Criterion. As Table 3.1 indicates, the noise can be correlated with the amount of photons that are emitted from the intensifying screen. Therefore, as the energy and quantity of x-rays is reduced, the images' SNR will approach 5 (Rose's Criterion).

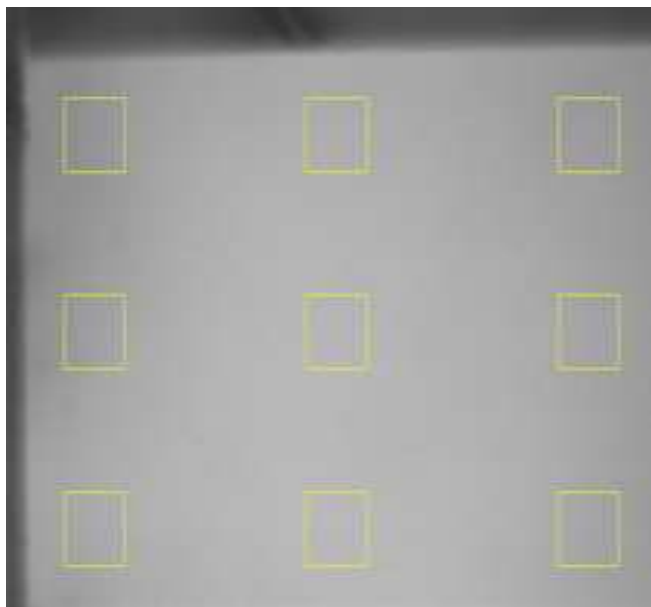


Figure 4-1: Each yellow square indicates where a signal and noise measurement was taken. The image above is of an intensifying screen at 50kV/79 μ A.

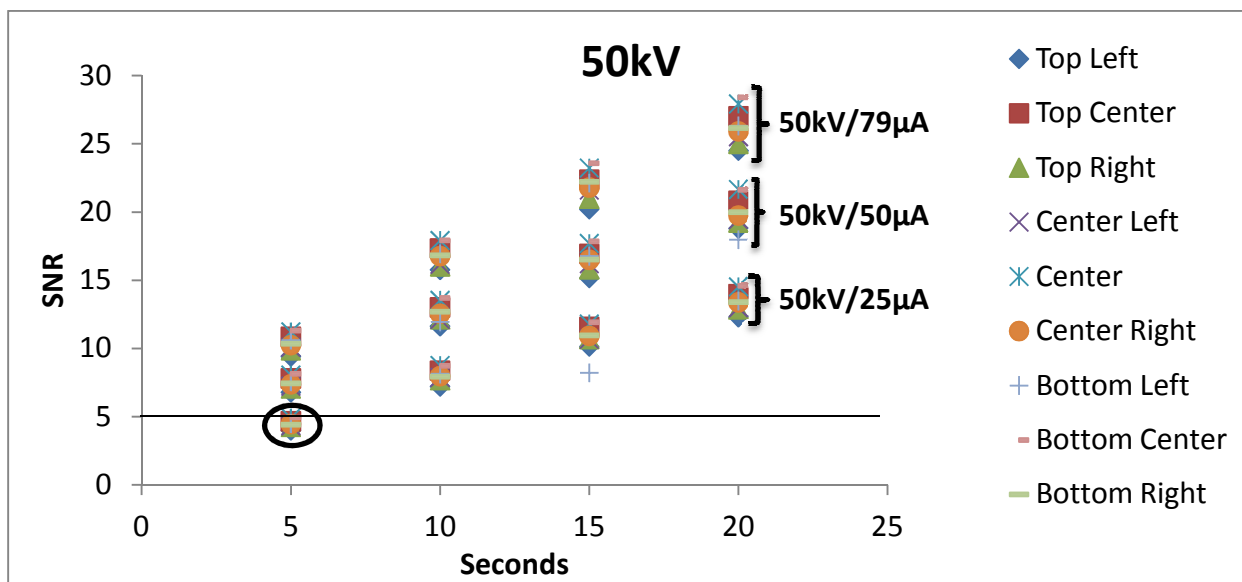


Figure 4-2: As the quantity of x-rays is reduced, the SNR decreases since there are fewer photons being acquired by the CCD camera. However, all three above settings adhere to Rose's Criterion except for the circled data. The black line that intersects a SNR of 5 is where objects are 100% discernible. Above the line indicates images comply with Rose's Criterion.

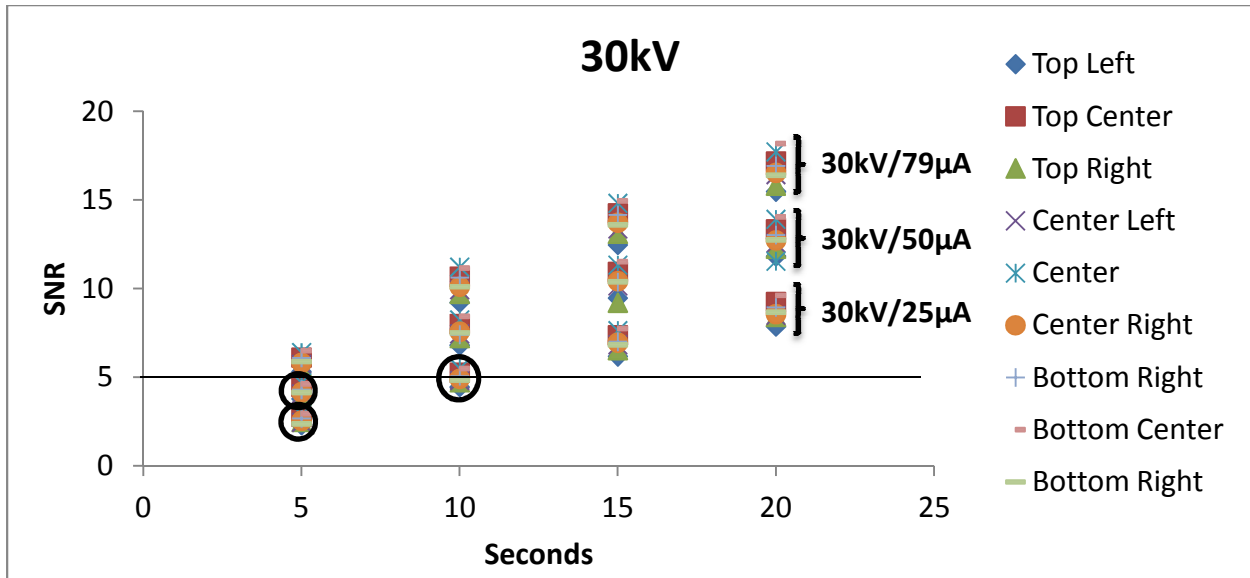


Figure 4-3: As the voltage is reduced, the energy of the x-rays is reduced which in turn reduces the number of photons being emitted from the intensifying screen. As the light output decreases, the image signal is reduced and the noise increases. All but the three circled data groups adhere to Rose's Criterion (black line).

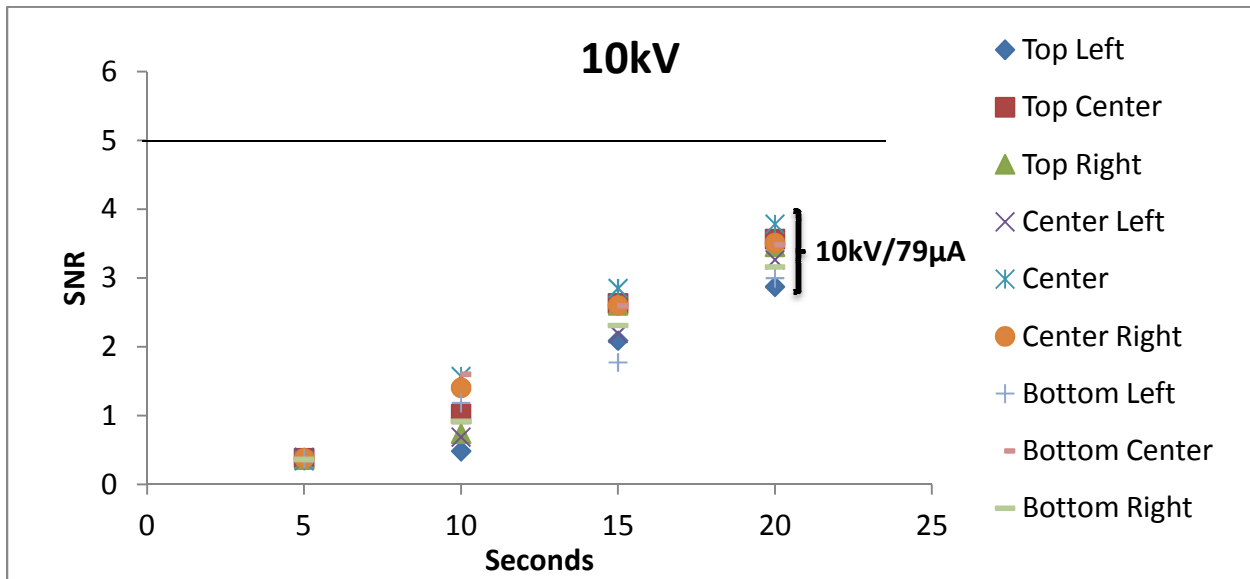


Figure 4-4: All of the images given above do not exceed the line intersecting a SNR of 5. There are not enough photons coming from the intensifying screen in order to make images 100% discernible. Consequently, at the exposure times given, Rose's Criterion (black line) is not met and should not be used with this DRS.

From Figures 4-2, 4-3, and 4-4, it is apparent that the number of x-rays striking the intensifying screen has a large impact on the SNR. As the quantity of x-rays is reduced, the SNR is decreased until it approaches Rose's Criterion, which we have defined as the lower limit of the SNR for producing useful images with our DRS. Therefore, a 10kV energy should not be used with our DRS since it cannot produce images with a SNR of or greater than 5 for any usable exposure time. Since dose is not a factor in our DRS, longer exposure times could be tested to find if 10kV could produce a discernible image. However, operating the x-ray source for extended periods of time heats up the x-ray filament and can cause the beam to be unstable or worse; the circuitry to malfunction. Therefore, from these results we can determine that energies ranging from 30kV to 50kV and a tube current of above ~79 microAmps (10-20 second exposure) should be used with our DRS.

4.2 Spatial Resolution Results

When defining spatial resolution, Modulation Transfer Function (MTF) is often used to quantify the transfer of contrast from the object to the image. That is to say, how well can our detection system reproduce the detail of an object that is being imaged? Using the MTF curve along with a line pair test phantom (as described in Chapter 3) will give us an idea of the limitations of the spatial resolution of a DRS.

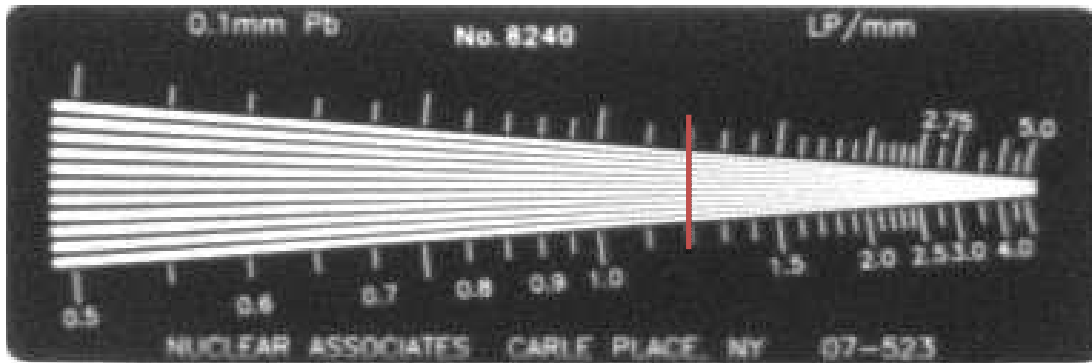


Figure 4-5: An image of the line pair phantom using 50kV/79 μ A. At about 1.2 LP/mm (red line) the lines blur together such that they are no longer distinguishable as separate lines. This observation is biased by the viewers' perspective and differences in their vision.

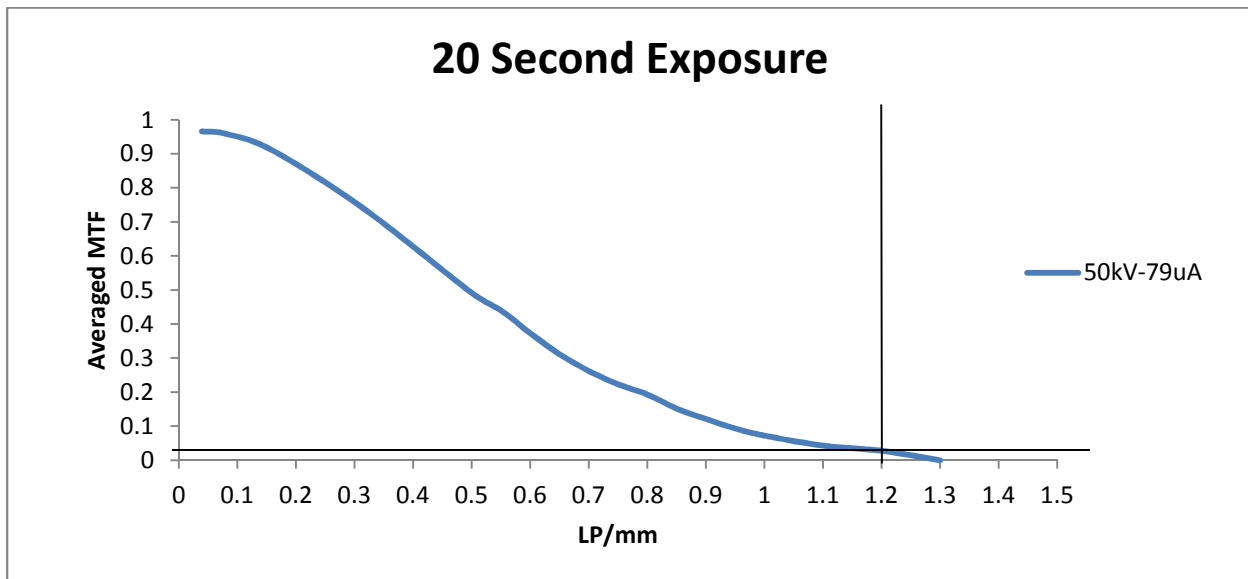


Figure 4-6: The Modulation Transfer as a function of spatial frequency (line pairs per millimeter). The intersection of the horizontal and vertical black lines indicates where the lines begin to visually blur together on Figure 4-5 (1.2 LP/mm).

An image of a line pair phantom taken at the optimal SNR settings determined in section 4.1 (50kV/79 μ A and 20 second exposure), is shown in Figure 4-5, with the MTF for this image plotted in Figure 4-6. A MTF value of 1 indicates all of the contrast has been transferred from the object to the image, while 0 indicates no contrast is transferred. This means that at a spatial frequency of 1.2 LP/mm approximately 3% of contrast is transferred, which represents the minimum contrast needed to resolve small objects with our DRS. At 1.3LP/mm, no contrast has been transferred and the lines from Figure 4-5 begin to blur together.

The spatial resolution limitations of our DRS are illustrated in Figure 4-5 and 4-6. Using optimal settings, (50kV/79 μ A with a 20 second exposure) the line pair phantom shows the maximum spatial resolution capabilities that can be resolved using our DRS given by the relationship:

$$f = \frac{1}{2\Delta} = 1.2 \text{ LP/mm}$$

$$\text{Object Size} = \frac{1}{2f} = 0.42\text{mm.}$$

As the x-ray energy (and thus penetrating power of the x-rays) is reduced, the transfer of contrast and spatial resolution decreases as seen in Figures 4-7 and 4-8. This decrease in contrast is due to a sharp decrease in measured signal. As the x-ray energy is reduced, the signal decreases to a point that the noise in our system becomes overwhelming at ~20kV/79 μ A, as shown in Figure 4-9. At 10kV-79 μ A, the x-rays are unable to penetrate the lead/plastic mixture of the line pair phantom and the images (not shown) appeared as one darkened rectangle.

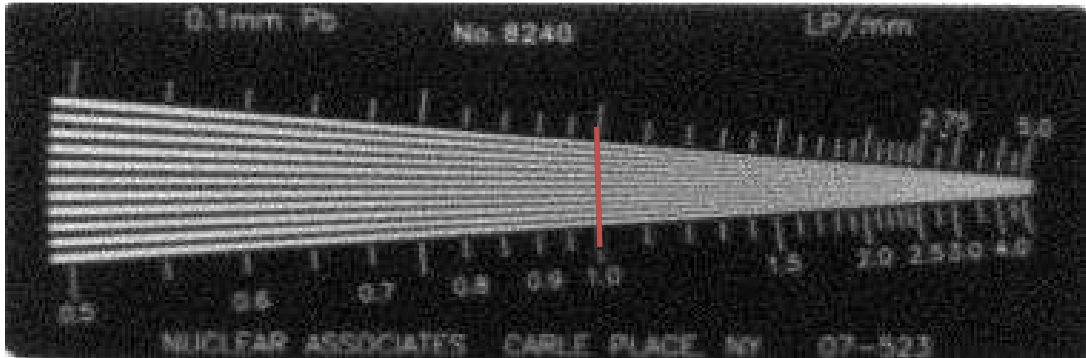


Figure 4-7: As the penetrating power of the x-rays decrease, the ability to identify smaller objects becomes more difficult. This image at 30kV/79 μ A has a slightly lower resolution limit (red line) than seen for 50kV/79 μ A.

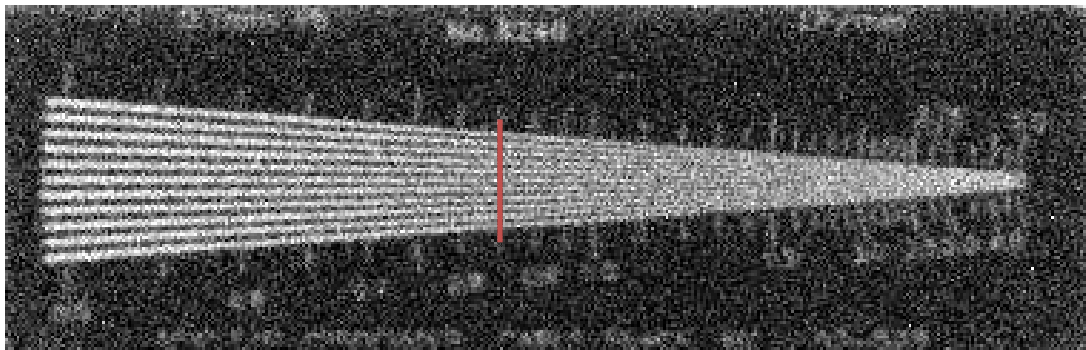


Figure 4-8: As we continue to reduce the penetrating power of the x-ray beam (20kV/79 μ A), the noise continues to increase. The white specs (noise) and the increase of blurring between line pairs in the image greatly reduces the upper limit of resolvable spatial frequency. At about 0.85 LP/mm (red line) is where the lines begin blurring together making objects of about 0.6 mm the smallest that are identifiable.

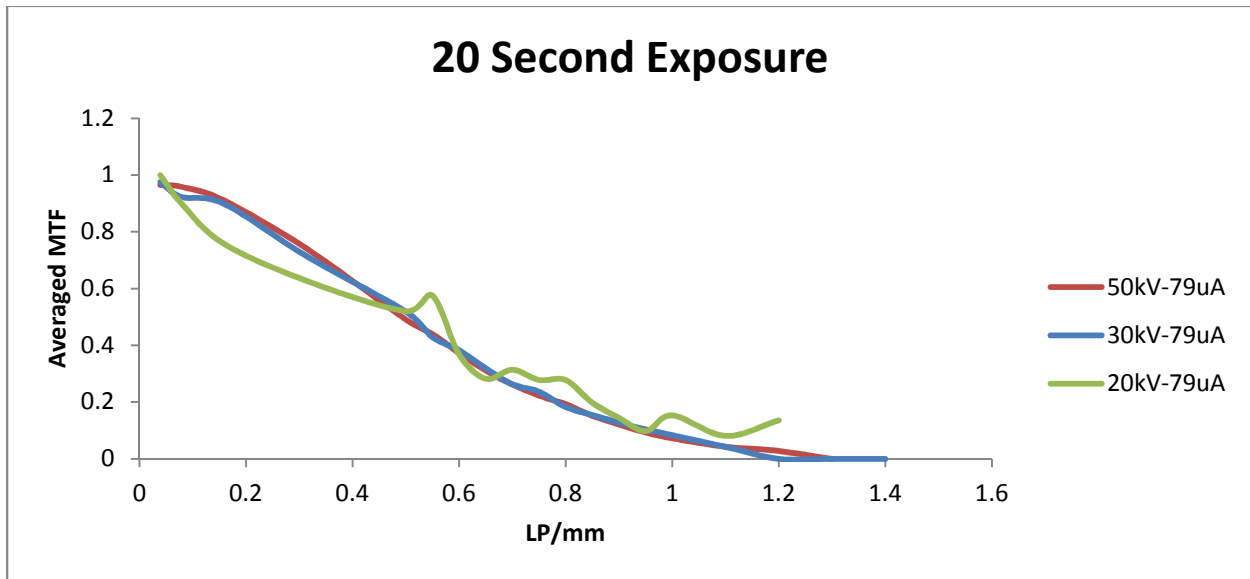


Figure 4-9: As the penetrating power of the x-rays decrease, the line pairs starts to become indifferntiable at increasing spatial frequency.

The smallest object that can be indentified in an image produced by our DRS is approximately 0.42mm with an x-ray tube setting of 50kV and 79 μ A. As the energy and quantity of x-rays decrease, fewer photons from the intensifying screen will strike the CCD camera, thus increasing the noise and reducing the acheivable spatial resolution. As the light output from the screen decreases, images become nosier, making it more difficult to extract useful information. Therefore, if small objects need to be identified in an image, it would be useful to use the 50kV/79 μ A setting to increase the the light output from the intinsifying screen, in turn increasing the spatial resolution acheivable with the DRS.

4.3 Contrast Results

When determining the different levels of contrast in an image, it is important to have an image that contains objects of a known thickness and density giving different levels of contrast. This will help show how the contrast provides a clear image and what the minimum contrast an object may have and still be visible when taken with our DRS. A contrast-detail phantom is shown in Figure 4-10. This phantom contains a series of foam rubber squares

(density = $0.0001 \frac{\text{g}}{\text{mm}^3}$) ranging in size from $3 \times 3 \text{ mm}^2$ to $40 \times 40 \text{ mm}^2$ and with a thickness ranging from 2 mm to 10 mm. Contrast is based on object composition, and since the foam rubber used for this contrast-detail phantom has a very low density, the low energy x-rays from the DRS can easily penetrate through it. As the voltage is decreased, the contrast between the foam squares increased. This is due to x-rays being absorbed by the foam (Figure 4-11). As the x-ray tube voltage is continually reduced, the absorption of the x-rays in the foam square phantom continues to increase but the clarity of the image begins to falter (Figure 4-10). Even though the contrast is increasing to help better define the low density squares, the noise is increasing and the spatial resolution is decreasing, making the image quality be reduced. Image 1 in Figure 4-10 shows the variety of thickness between each column of squares, whereas image 2 shows a stronger contrast between each column. Image 3 becomes too difficult to extract information from due to the increased noise and decreased spatial resolution. Therefore, when extracting information about low density materials, a compromise must be met in order to find the appropriate settings for a quality image.

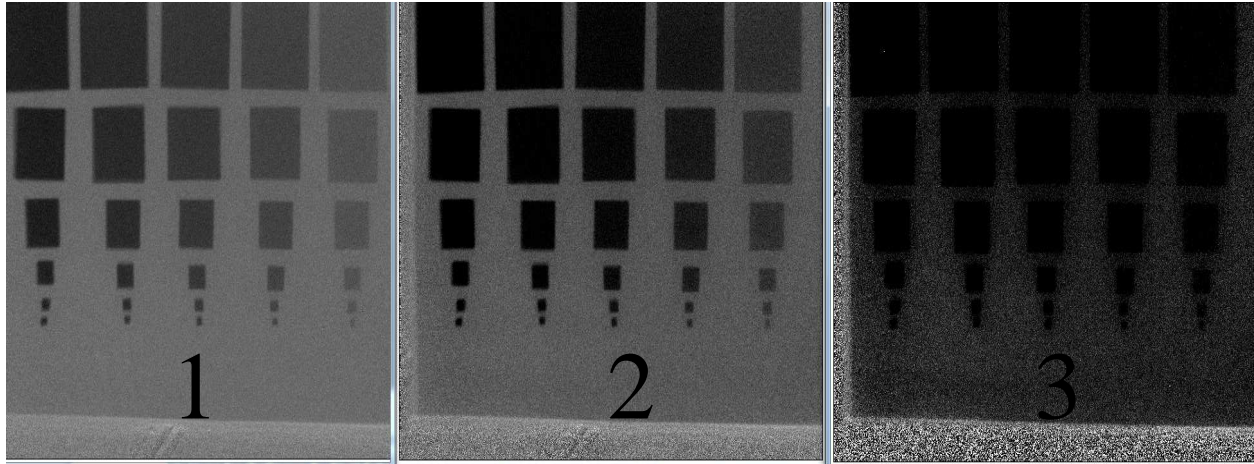


Figure 4-10: As the x-ray energy is decreased (50kV/79 μ A (1), 30kV/79 μ A (2), 20kV/79 μ A (3)) more x-rays are absorbed by the foam, thus increasing the contrast.

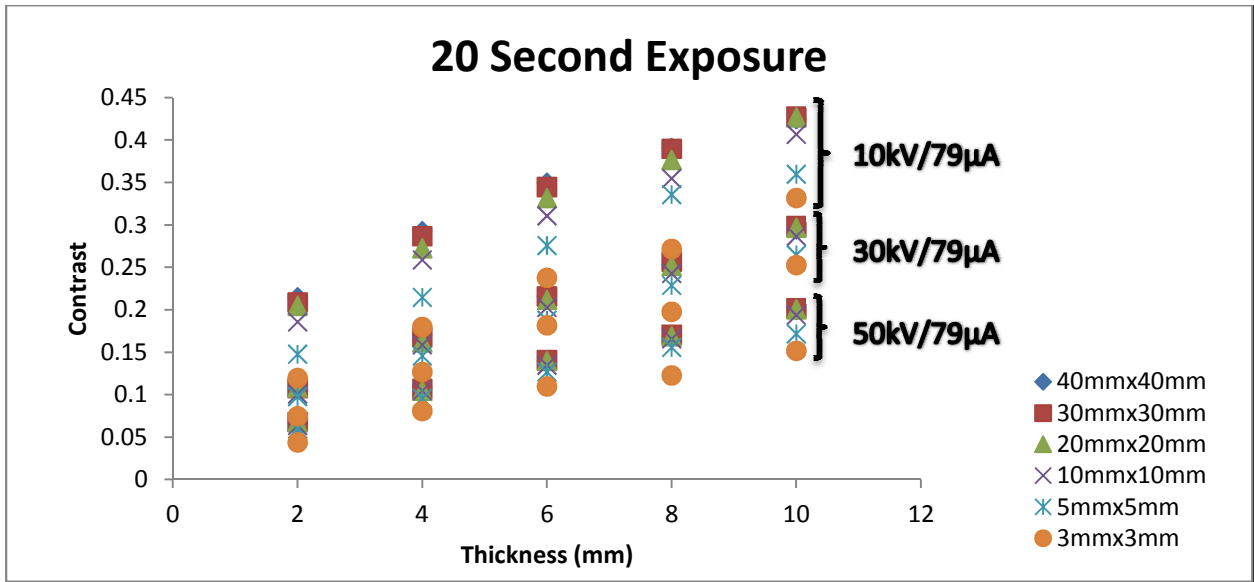


Figure 4-11: As the x-ray energy is reduced, the contrast between each square is increased. The energy needed for an image depends on what the object is comprised of, as well as the size of the object.

4.4 Combining the Three Tests (Noise, Spatial Resolution, and Contrast)

Once the images have been acquired; noise, spatial resolution, and contrast are used together to gather information from an image. The images of two objects, shown in Figure 4-12, are used to show how noise, spatial resolution, and contrast have an effect on extracting information. Figure 4-12 shows a motherboard from a Dell PC (left) and an outline of Pistol Pete with an OSU emblem (right). These objects have been imaged with our DRS to see if the intensity values give any information as to the identity of the objects.

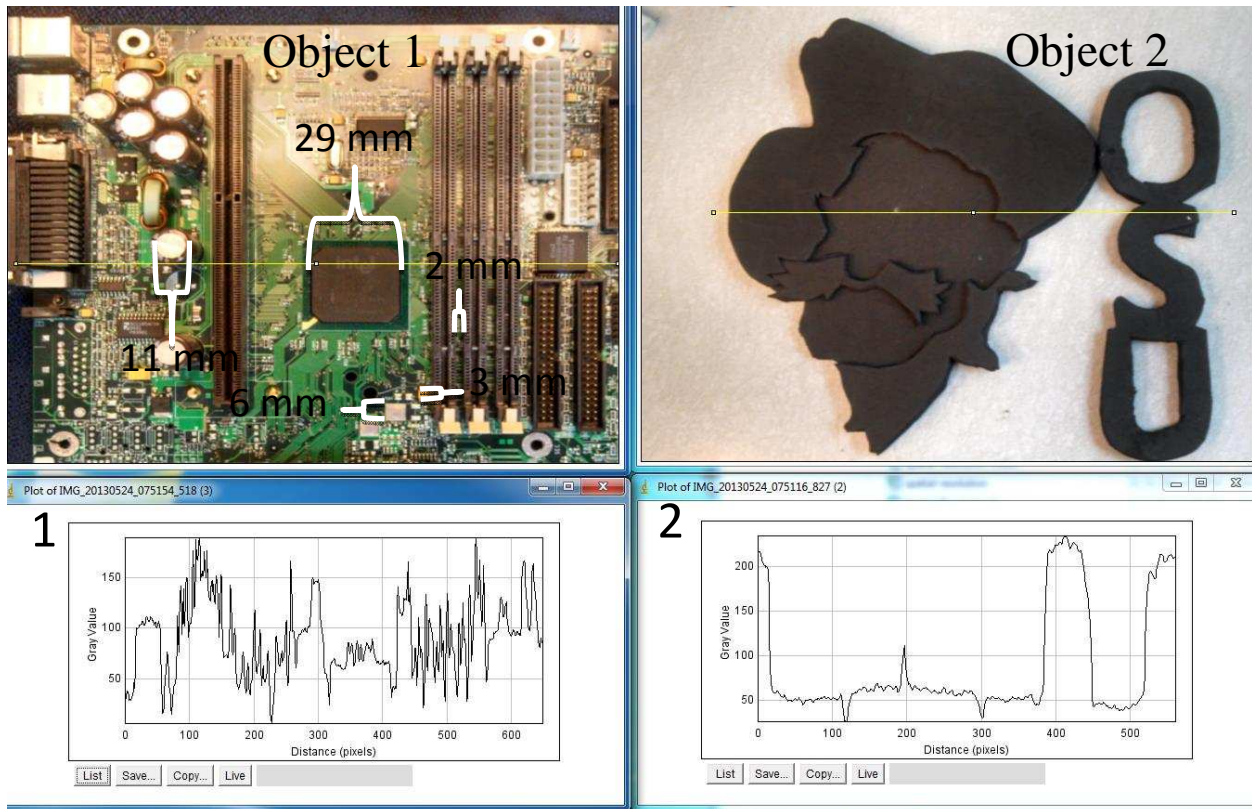


Figure 4-12: Images of a computer motherboard (Object 1) and a foam rubber “Pistol Pete” cutout (Object 2). Labeled are the sizes of several objects identifiable in images taken of these objects with the DRS.

(1) 50kV/79 μ A (2) 30kV/79 μ A (3) 10kV/79 μ A

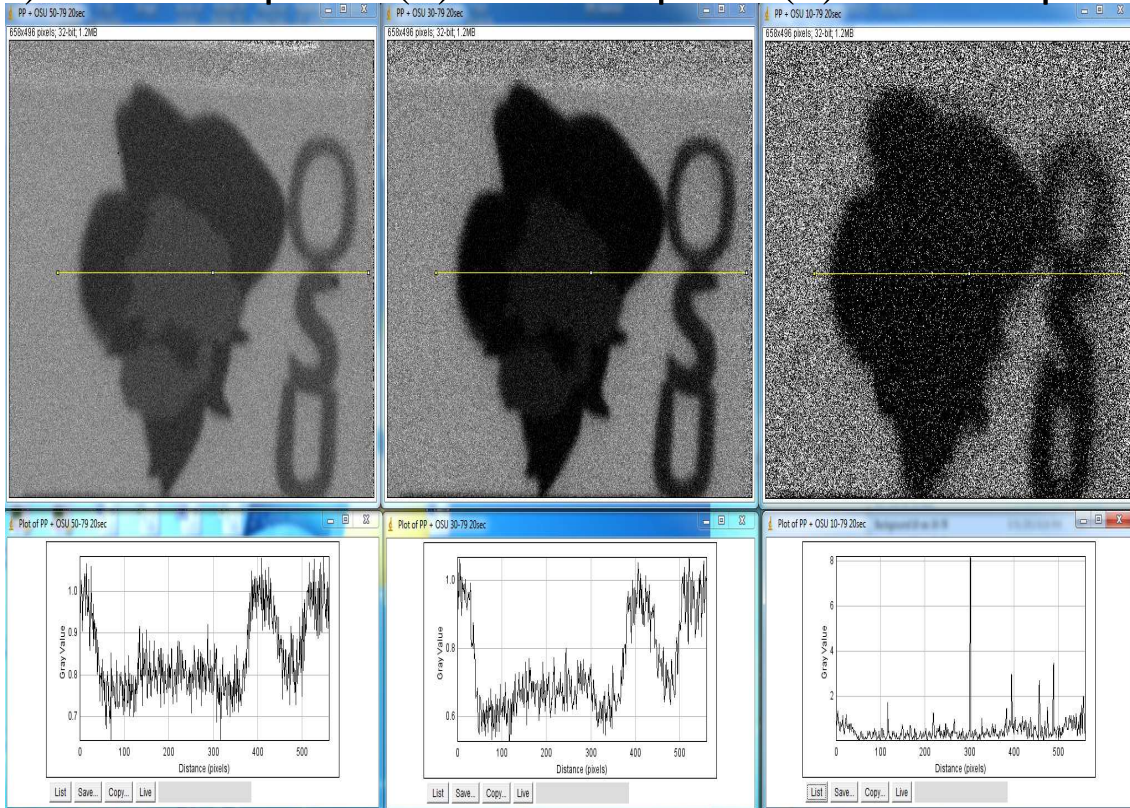


Figure 4-13: In this 20 second exposure, the x-ray energy is reduced (from left to right) and the noise increases to a point where the image is difficult to identify. Also, due to the foam absorbing more x-rays as the energy is decreased, the contrast is increased and may offer a clearer image, such as in image 2. Only an outline of Pistol Pete in image 3 is recognizable as compared to image 1.

(1) 50kV/79 μ A (2) 30kV/79 μ A (3) 10kV/79 μ A

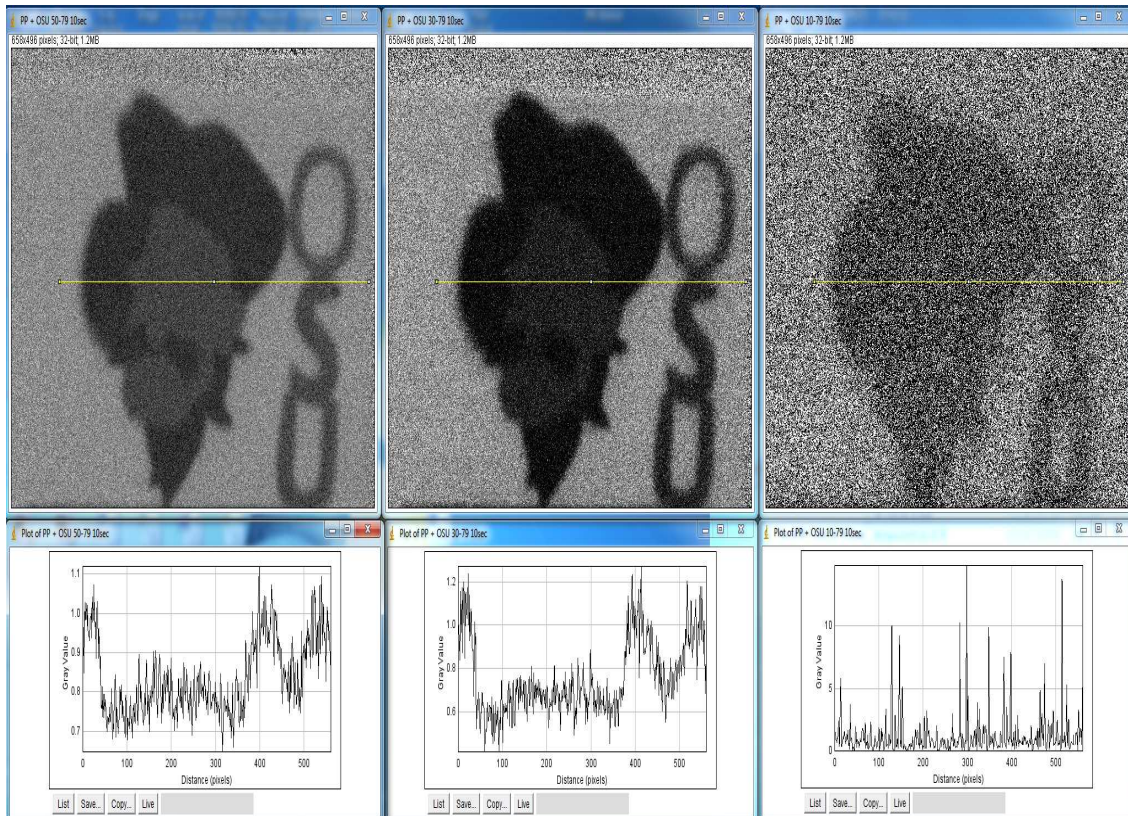


Figure 4-14: The quantity of x-rays was reduced by decreasing the exposure time to 10 seconds. The contrast changes as the energy decreases to a point where only an outline is observable (image 3). The noise increases as the energy is decreased to a point where the image is difficult to extract any kind of information.

Object 2 from Figure 4-12 uses mainly contrast to help extract the image of Pistol Pete when using our DRS. Known for his thick mustache, cowboy hat, and handkerchief; Pistol Pete is highlighted in foam using thicker foam segments for his signature look. As the output of light from the intensifying screen decreases, Pistol Pete becomes more difficult to distinguish.

Object 1 is a Dell PC motherboard comprised of various components. Image 1 (Figure 4-15) shows the different attenuation through the different components of the motherboard. Also, the spatial resolution is greater at 50kV/79 μ , as seen in Figure 4-5; therefore, smaller objects are able to be identified in image 1 and 4 (Figures 4-15 and 4-16). As the energy of the x-rays decrease, the images begin to be unidentifiable and just an outline is able to be distinguished. The smallest object that is identifiable in image 1 and 4 is a 2mm gap between the memory card holders. Arrows in image 1 and 4 show the small portions of the motherboard that are observable and are measured in Figure 4-12. The x-rays are continually being attenuated through the different components of the motherboard, decreasing the light output from the intensifying screen until each component of the motherboard is reduced to the same pixel value (image 5). It is difficult to point out the different components in image 5 as opposed to image 1 due to the light output of the screen. Also, as the light output of the intensifying screen decreases, the noise will increase to a point where the image is unrecognizable, such as image 3 and 6.

(1) 50kV/79 μ A (2) 30kV/79 μ A (3) 10kV/79 μ A

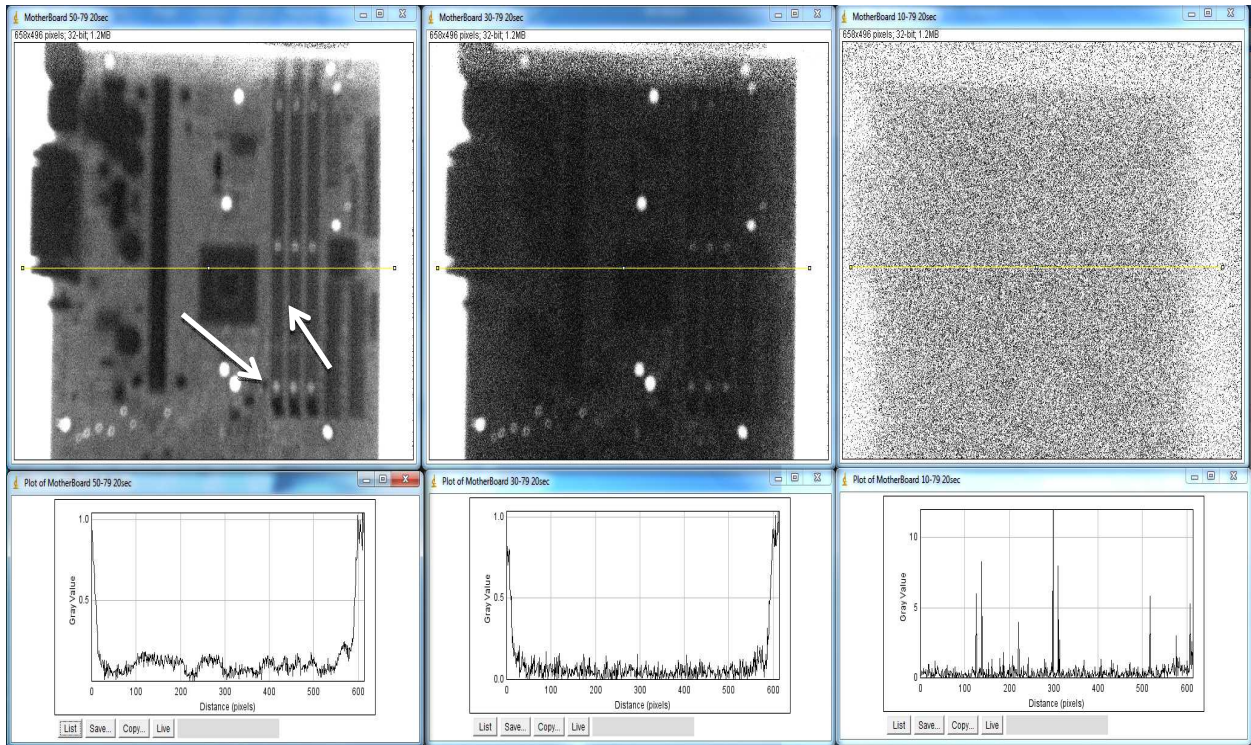


Figure 4-15: A 20 second exposure at different voltages was taken to determine what information could be extracted from each image.

(4) 50kV/79 μ A

(5) 30kV/79 μ A

(6) 10kV/79 μ A

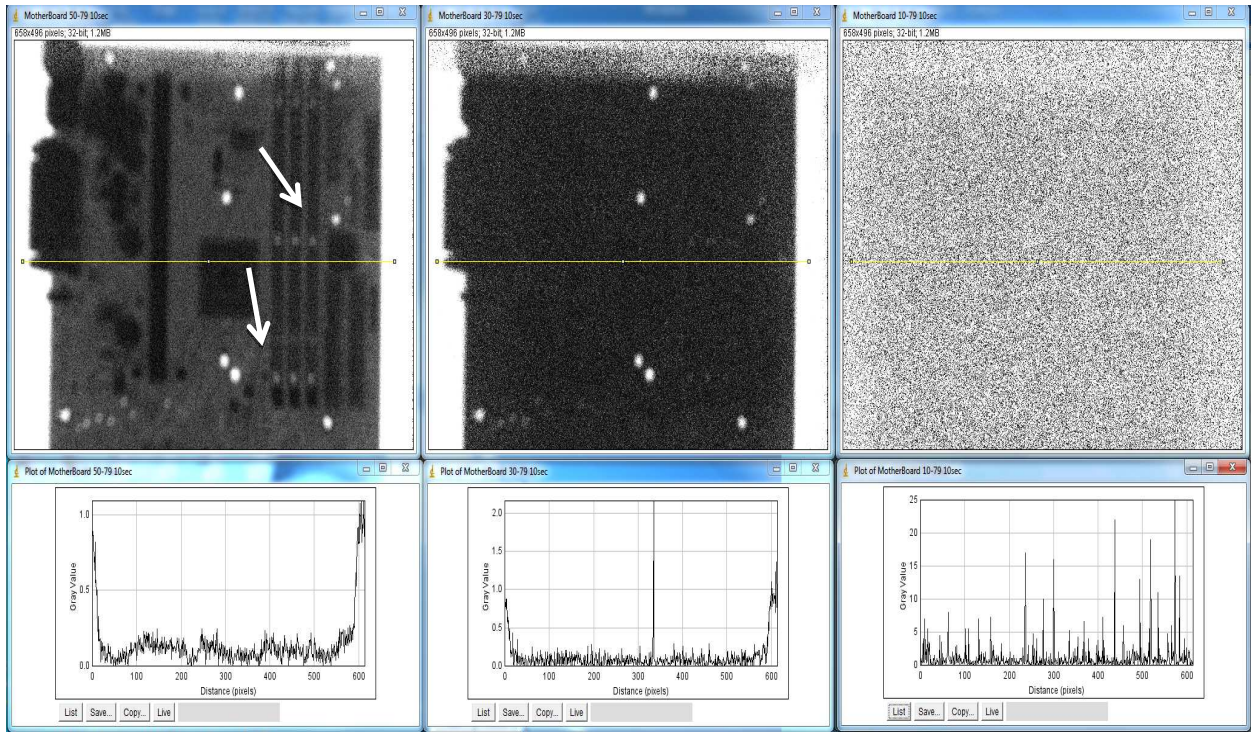


Figure 4-16: The exposure time was lowered to 10 seconds to see if the same information could be extracted as Figure 4-15.

Chapter 5 – Conclusion

5.1 Goal of this Project


The primary goal of this study was to provide a cost efficient digital radiography system that can be used in an educational setting. The ability to build teaching instruments such as a DRS can provide valuable hands-on experience for students learning the basic physical principles of Diagnostic Imaging. The simple tests shown in previous chapters were designed to test and characterize the limits of our DRS. At optimal settings (50kV/79 μ A, 20 second exposure), our DRS can detect roughly 0.42mm sized objects with a SNR of approximately 25. As for contrast, the composition of the object must be taken into consideration when choosing what settings are necessary for extracting information from an image. As the x-ray energy is increased, fewer x-rays are being absorbed by the object; thus changing the contrasts between components of different composition and density in the object. The optimal settings are able to provide images with the best levels of noise, spatial resolution, and contrast. However, when the energy and quantity of x-rays are altered, the principles of medical imaging start to become evident. For example, as the energy or amount of x-rays is decreased, it can be shown that the noise and the attenuation through the sample foam phantoms used for the experiment increases. These principles are crucial to understanding how a DRS is able to provide an informative image. If the energy or quantity of x-rays is lowered to a point where the SNR falls below 5, we know that from Rose's Criterion the object will not necessarily be identifiable 100% of the time. Therefore, the DRS would not be capable of producing reliable and usable images.

5.2 Cost of DRS

The total cost of our DRS was approximately \$17,000.00 with the majority of the expenses going into the Luca S CCD camera (~\$10,000). The x-ray source was purchased from Amptek for \$6,500.00. The intensifying screens and lens for the CCD camera were available as surplus items within the department of Physics at OSU. The final \$500 in expenses went to the lead and wood used to construct the housing unit. All imaging analysis software was either free, such as imageJ, or available through the OSU site license such as Microsoft Excel and Labview. Andor provided a labview program to run the camera and save the images. The images from our DRS could be exported from Labview to imageJ for analysis and the extracted data finally imported into Microsoft Excel to help further analyze the characteristics of our DRS. Therefore, all software used to help analyze our DRS images is easily accessible and for the most part free. The Luca S camera could be operated using a variety of programs; however, since a copy of Labview was already installed in the lab and ready to use, it was chosen to operate the camera.

5.3 Building a More Cost Efficient DRS

Although the cost for our DRS was around \$17,000.00, a variety of changes in designing a DRS can be made to significantly lower the cost. Replacing the main components of our DRS (x-ray source, intensifying screens, and camera) can reduce the cost, and possibly the limitations. For example, when looking for affordable x-ray sources, Ebay offers a variety of portable dental x-ray machines for sale. Currently an x-ray source, as seen in Figure 5-1, is listed on the Ebay website for approximately \$600.00, although prices may vary.



PORTABLE DENTAL X-RAY MACHINE

DENTAL PORTABLE DIGITAL X RAY MACHINE SYST BOX!!!

Item: **New**
 condition:
 Time left: 6h 56m 26s (Jun 09, 2013 22:27:01 PDT)
 Quantity: 5 available

Price: **US \$579.00** [Buy It Now](#)
[Add to cart](#)
[Add to Watch list](#)

BillMeLater: Spend \$99+ and get 6 months to pay
 Subject to credit approval. [See terms](#)

Shipping: **\$109.00** Expedited Shipping | [See details](#)
 Item location: Lithonia, Georgia, United States
 Ships to: **Worldwide**

Figure 5-1: Ebay offers a variety of dental x-ray machines (example seen above). The limitations of the above x-ray source are quite different than the limitations of the Amptek x-ray source provided in our DRS. This x-ray source has a higher energy potential (70kVp) a set current (0.5mA) and a maximum exposure time of 10 seconds. The DRS would need to be set up according to the limitations of both the x-ray source and camera.



Orion StarShoot AutoGuider
 by [Orion](#)
 ★★★★★ (3 customer reviews) | [Like](#) (0)

Price: ~~\$279.99~~
 Sale: **\$237.99**
 You Save: **\$42.00 (15%)**

In Stock.
 Ships from and sold by [Orion Telescopes & Binoculars](#).

Figure 5-2: The Orion Starshoot Autoguider is a CCD camera typically used for imaging the night sky. However, ignoring the autoguider feature, the camera can be set up on any basic PC in order to take immobile images. Lenses can be purchased on the Orion website to accommodate the setup required for the DRS.

To further reduce the cost of the DRS, the next option is to replace the CCD camera. An assortment of CCD cameras can be used to collect the light coming from the intensifying screen. First, the CCD camera needs to have an exposure time equal to or greater than the exposure time of the x-ray source. Second, the camera needs the ability to be controlled by a PC that is located at a safe distance from the x-ray source. The online retailer Amazon sells astronomy CCD cameras for approximately \$240.00 (Figure 5-2).

Finally, the intensifying screens can be acquired from several sources for a relatively inexpensive price. A cassette used for film radiography can be purchased as well on Ebay for roughly \$50.00. Cassettes can range in size and can be selected according to the dimensions of the DRS. The housing and wiring of the DRS, essentially does not range greatly in price; therefore, the price of both will depend on the size of the DRS. Assuming that the newly assembled DRS will be approximately the same size as our DRS, the total cost would come to be around \$500.00. The total cost of this newly acquired, cost efficient DRS is ~8.8% of the cost of our current DRS and ~1.2% of the cost of the commercial portable x-ray system offered by Absolute Medical Equipment described in Chapter 1.

5.4 Future Work

Future experiments with our DRS consist of transforming it into what is essentially a CT scanner. By doing this, the only additional physical component needed would be a variable rotating stage where the object can be located. Instead of the x-ray source rotating around the object, as per normal CT scanners, the object would rotate while the x-ray source is in a fixed location. The object would rotate and images would be taken. Additional software would be needed to reconstruct the 2D intensity images into a tomographic attenuation image.

Also, additional work should include characterization of the amount of light output per energy/current and exposure time. This would help find the limitations of noise as a function of photons hitting the CCD chip. Therefore, if the number of photons hitting the camera were known, then the minimum settings could be found to produce an image with an SNR of or above 5. Additionally, most of the photons coming from the intensifying screen are wasted due to the fact that they are emitted isotropically and only a small portion of photons from the intensifying screen interact with the CCD chip. In conclusion, to make the DRS more efficient, a setup involving construction of an apparatus directing the maximum amount photons onto the CCD chip would be beneficial.

References

- Bansal, G. J. (2006). "Digital radiography. A comparison with modern conventional imaging." Postgrad Med J **82**(969): 425-428.
- Bushberg, Jerrold, Anthony Seibert, Edwin Leidholdt, and John Boone. (2002). The Essential Physics of Medical Imaging. Philadelphia: Lippincott Williams & Williams.
- Carlton, R. A., Arlene (2001). Principles of Radiographic Imaging. Albany, NY, Delmar.
- Chotas, H. G., J. T. Dobbins, 3rd and C. E. Ravin (1999). "Principles of digital radiography with large-area, electronically readable detectors: a review of the basics." Radiology **210**(3): 595-599.
- Frame, P. "Tales from the Atomic Age." 2013, from <http://www.orau.org/ptp/articlesstories/invisiblelight.htm>.
- Griffiths, M. "Radiographic Science." X-ray Production, 2013, from http://hsc.uwe.ac.uk/radscience/xray_prod/production_of_xrays03_files/frame.htm.
- Hill, D. R., Ed. (1975). Principles of Diagnostic X-ray Apparatus. New York, Macmillan.
- MMD (Modus Medical Devices). (2011), Lab 3; Spatial Resolution and Modulation Transfer Function, DeskCat Student Lab Exercises, London, Ontario.
- NIH (National Institute of Health). ImageJ, 2013, from <http://rsbweb.nih.gov/ij/>.
- Oldnall, N. J. (1999). "Intensifying Screens." 2013, from <http://www.e-radiography.net/nickspdf/Screens.PDF>.
- Siemens. (2012). "Understanding Medical Radiation." Radiography (Plain X-rays), 2013, from <http://www.medicalradiation.com/types-of-medical-imaging/imaging-using-x-rays/radiography-plain-x-rays/>.
- Sprawls, P. Interaction of Radiation with Matter, 2013, Sprawls Educational Foundation. From <http://www.sprawls.org/ppmi2/INTERACT/>.

Suetens, P. (2002). Fundamentals of Medical Imaging. New York, NY, Cambridge University Press.

van der Stelt, P. F. (2008). "Better imaging: the advantages of digital radiography." J Am Dent Assoc **139 Suppl**: 7S-13S.

USNLM (U.S. National Library of Medicine), Dream Anatomy, 2013, from https://www.nlm.nih.gov/dreamanatomy/da_g_Z-1.html.

USNRC (U.S. Nuclear Regulatory Commission). Radiological Toolbox, 2013, from <http://www.nrc.gov/about-nrc/regulatory/research/radiological-toolbox.html>

Vita

Christopher Glen Brown

Candidate for the Degree of

Masters of Science

Thesis: BUILDING A COST EFFICIENT DIGITAL RADIOGRAPHY SYSTEM FOR EDUCATIONAL PURPOSES

Major Field: Physics with Option in Medical Physics

Biographical:

Education: Received Bachelor of Science in Physics at Henderson State University, Arkadelphia, AR in May 2010. Completed the requirements for the Master of Science degree with major in Physics (Medical Option) at Oklahoma State University, Stillwater, OK in July 2013.

Experience: Interned at St. Johns in Tulsa, Oklahoma Summer 2013.

Professional Memberships: AAPM